






Review

# Imaging Features of Post Main Hepatectomy Complications: The Radiologist Challenging

Carmen Cutolo <sup>1</sup>, Federica De Muzio <sup>2</sup>, Roberta Fusco <sup>3</sup>, Igino Simonetti <sup>4</sup>, Andrea Belli <sup>5</sup> , Renato Patrone <sup>5</sup> ,  
Francesca Grassi <sup>6,7</sup>, Federica Dell'Aversana <sup>6</sup>, Vincenzo Pilone <sup>1</sup>, Antonella Petrillo <sup>4</sup> , Francesco Izzo <sup>5,†</sup>   
and Vincenza Granata <sup>4,\*,†</sup> 

- <sup>1</sup> Department of Medicine, Surgery and Dentistry, University of Salerno, 84084 Fisciano, Italy; carmencutolo@hotmail.it (C.C.); vpilone@unisa.it (V.P.)
  - <sup>2</sup> Department of Medicine and Health Sciences V. Tiberio, University of Molise, 86100 Campobasso, Italy; demuziofederica@gmail.com
  - <sup>3</sup> Medical Oncology Division, Igea SpA, 80013 Naples, Italy; r.fusco@igeamedical.com
  - <sup>4</sup> Radiology Division, Istituto Nazionale Tumori—IRCCS—Fondazione G. Pascale, Via Mariano Semmola, 80131 Naples, Italy; igino.simonetti@istitutotumori.na.it (I.S.); a.petrillo@istitutotumori.na.it (A.P.)
  - <sup>5</sup> Hepatobiliary Surgical Oncology Division, Istituto Nazionale Tumori—IRCCS—Fondazione G. Pascale, Via Mariano Semmola, 80131 Naples, Italy; a.belli@istitutotumori.na.it (A.B.); dott.patrone@gmail.com (R.P.); f.izzo@istitutotumori.na.it (F.I.)
  - <sup>6</sup> Division of Radiology, Università degli Studi della Campania Luigi Vanvitelli, 81100 Naples, Italy; francesca.grassi1@studenti.unicampania.it (F.G.); federica.dellaversana@studenti.unicampania.it (F.D.)
  - <sup>7</sup> Italian Society of Medical and Interventional Radiology (SIRM), SIRM Foundation, Via della Signora 2, 20122 Milan, Italy
- \* Correspondence: v.granata@istitutotumori.na.it  
† These authors contributed equally to this work.



**Citation:** Cutolo, C.; De Muzio, F.; Fusco, R.; Simonetti, I.; Belli, A.; Patrone, R.; Grassi, F.; Dell'Aversana, F.; Pilone, V.; Petrillo, A.; et al. Imaging Features of Post Main Hepatectomy Complications: The Radiologist Challenging. *Diagnostics* **2022**, *12*, 1323. <https://doi.org/10.3390/diagnostics12061323>

Academic Editor: Jung-Gil Park

Received: 9 May 2022

Accepted: 25 May 2022

Published: 26 May 2022

**Publisher's Note:** MDPI stays neutral with regard to jurisdictional claims in published maps and institutional affiliations.



**Copyright:** © 2022 by the authors. Licensee MDPI, Basel, Switzerland. This article is an open access article distributed under the terms and conditions of the Creative Commons Attribution (CC BY) license (<https://creativecommons.org/licenses/by/4.0/>).

**Abstract:** In the recent years, the number of liver resections has seen an impressive growth. Usually, hepatic resections remain the treatment of various liver diseases, such as malignant tumors, benign tumors, hydatid disease, and abscesses. Despite technical advancements and tremendous experience in the field of liver resection of specialized centers, there are moderately high rates of postoperative morbidity and mortality, especially in high-risk and older patient populations. Although ultrasonography is usually the first-line imaging examination for postoperative complications, Computed Tomography (CT) is the imaging tool of choice in emergency settings due to its capability to assess the whole body in a few seconds and detect all possible complications. Magnetic resonance cholangiopancreatography (MRCP) is the imaging modality of choice for delineating early postoperative bile duct injuries and ischemic cholangitis that may arise in the late postoperative phase. Moreover, both MDCT and MRCP can precisely detect tumor recurrence. Consequently, radiologists should have knowledge of these surgical procedures for better comprehension of postoperative changes and recognition of the radiological features of various postoperative complications.

**Keywords:** hepatectomy; postoperative complications; radiologists

## 1. Introduction

Liver resection is still the most efficient treatment of primary liver malignancies, including hepatocellular carcinoma (HCC) and cholangiocarcinoma (CCA), and in metastatic disease, such as colorectal liver metastases [1–9]. According to the increase in occurrence of these primary and metastatic cancers, the number of hepatic resections is globally rising, and it doubled in the USA from 1988 to 2000 [10,11]. The advancement in patient selection and the innovative surgical techniques have decreased the risk of mortality from 20% to 1–5% [12,13]. In spite of this, morbidity rates even now vary from 20 to 56%, depending on the patient characteristics, such as tumor size and localization, and multidisciplinary team

expertise and available technologies [12–15]. As reported by Benzoni et al., major hepatectomies, Pringle maneuver protracted more than 20 min and blood transfusions greater than 600 mL were associated with significant increases in complications. Furthermore, types B and C of the Child–Pugh classification and histopathologic grading are correlated with higher complications in patients with HCC [16]. Sadamori et al. [17] reported a prominently higher frequency of bile leakage (12.8% overall) and organ/space surgical site infections (8.6% overall) in patients undergoing repeat hepatectomy and prolonged surgery.

To summarize, increasing age with significant related comorbidities, extended resections, and iterative hepatectomies are all risk factors for the development of postoperative complications. Moreover, for colorectal metastasis, if, on one hand, a preoperative chemotherapy regimen converted the lesion previously believed unresectable to resectable, on the other hand, after chemotherapy, the liver is more subject to steatosis and steatohepatitis with greater frequency of postoperative complications [18–22].

Radiology plays a key role in the early discovery of postoperative complications. In fact, recent progress in diagnostic imaging modalities such as computed tomography (CT) [23–34] or magnetic resonance imaging (MRI) [35–48] with cholangiopancreatography have enabled an exact assessment of the postoperative morphological changes of the remaining liver, as well as a determination and an evaluation of postoperative complications [49–52].

The aim of this work is to summarize the main posthepatectomy complications and their radiological features.

## 2. Type of Resections

When discussing potential complications after liver resections, it is fundamental to specify the extent of the resection.

Liver resections (hepatectomies) can be categorized into anatomical and nonanatomical resections.

Anatomical resections consist of the removal of contiguous functional liver segments, while nonanatomic liver resections consist of the removal of the tumor with a margin of at least 1 cm without regard to segmental, sectional, or lobar anatomy [53–55]. Despite the number of segments removed, it is not enough to represent the complexity of a liver resection [56]; major hepatectomies are commonly defined as the resection of three segments in the left liver and four segments in the right liver.

The Terminology Committee of the International Hepato-Pancreato-Biliary Association defined a standardized nomenclature of anatomical resections in 2000 [57]. A right hepatectomy includes the removal of segments 5, 6, 7, and 8. It consists of the removal of all hepatic parenchyma to the right of the middle hepatic vein. An extended right hepatectomy (or right trisectionectomy) includes the additional resection of segment 4 (left medial section).

A left hepatectomy includes the removal of segments 2, 3, and 4 and consists of the removal of all hepatic parenchyma to the left of the middle hepatic vein. An extended left hepatectomy (or left trisectionectomy) involves the additional resection of segments 5 and 8 (right anterior section) [57]. Sectionectomies are defined by the type of section removed. A right anterior sectionectomy consists of the removal of the right anterior section—segments 5 and 8. A monosegmentectomy consists of the removal of a single segment, while a bisegmentectomy involves the resection of two contiguous segments [57]. Several studies demonstrated comparable morbidity in different types of liver resections, whereas others have shown significant differences in major hepatectomies. Zimmitti et al. [58] analyzed the incidence rates of postoperative complications in increasingly complex liver resections. They showed that, except for biliary leaks, the percentage of complications did not increase as the complexity of the operation increased. Li et al. [59] demonstrated that a major hepatectomy was related to greater rates of infectious (organ/space, superficial skin infections, pneumonia, sepsis, and septic shock), pulmonary (unplanned reintubation and prolonged ventilator support), renal (progressive renal insufficiency and acute renal failure), and

hematologic (bleeding within 72 h and deep venous thrombosis [DVT]) complications, when compared with minor hepatectomies [59].

A factor that should be considered is the pathology of the underlying liver. At least 80% of HCC patients will develop hepatic fibrosis or cirrhosis [60–68].

Accordingly, the remnant liver is already damaged and perhaps more vulnerable to further injury.

### 3. Complications

Complications, defined as any unexpected modification from a procedural course, and adverse events, described as any existent or potential injury connected with the treatment, could occur either during the procedure or after the procedure [69–73].

A major complication is an event that results in substantial morbidity and injury, allowing an increase in the level of care or resulting in hospital admission or a protracted hospital stay. Circumstances that are different from this condition are described as minor complications [69–73].

Postprocedural complications are a frequent occurrence after hepatic resections and differ based on the type of surgical procedure, the type of intervention on the biliary ducts and vascular structures, the grade and histological type of the treated tumor, and the existence of an underlying chronic disease [74–78]. According to the time of onset, postoperative complications can be defined as early and late complications. Fluid collection, vascular thrombosis, vascular or biliary duct damage, and diaphragmatic injuries are the most frequent early postoperative complications [74–78].

The most feared long-term complication is undoubtedly disease recurrence, while ischaemic cholangitis is a mild to severe late complication that could manifest months or even years after the procedure [79–83].

Complications should be assessed according to the following classification systems: (a) Common Terminology Criteria for Adverse Events standards, (b) Clavien–Dindo classification, (c) Society of Interventional Radiology classification, and (d) Cardiovascular and Interventional Radiological Society of Europe Quality Assurance Document and Standards for Classification of Complications [59]; complications should be classified constantly according to severity and time of incidence (e.g., intraprocedural, postprocedural, or late) [74–78].

Various imaging techniques could be used, alone or in association, to successfully assess patients after liver resection. The imaging techniques most commonly used in the detection and characterization of complications are Ultrasound (US) [84–87] and contrast-enhanced CT (CECT) [88–101].

In addition, Magnetic Resonance Imaging (MRI) is very important in the evaluation of late postoperative complications. In particular, MRI is fundamental in the early characterization of disease recurrence [102–113].

#### 3.1. Early Postoperative Complications

##### 3.1.1. Fluid Collection

Postsurgical fluid collection could be divided according to composition into hematomas (50%), bilomas (25%) (Figure 1), and abscesses (25%) (Figures 2 and 3) [114]. Collection usually tends to localize along the resection margins that should be carefully investigated during both US and CT examinations [115].

A biconvex or growing intraparenchymal areas, heterogeneous and echogenic on US or with a superfluid density value (between 50 and 60 HU) on unenhanced CT, are strongly suggestive of a hematoma [115]. The suspicion should be confirmed after the administration of a contrast medium agent since the hematoma does not show any contrast enhancement [115].

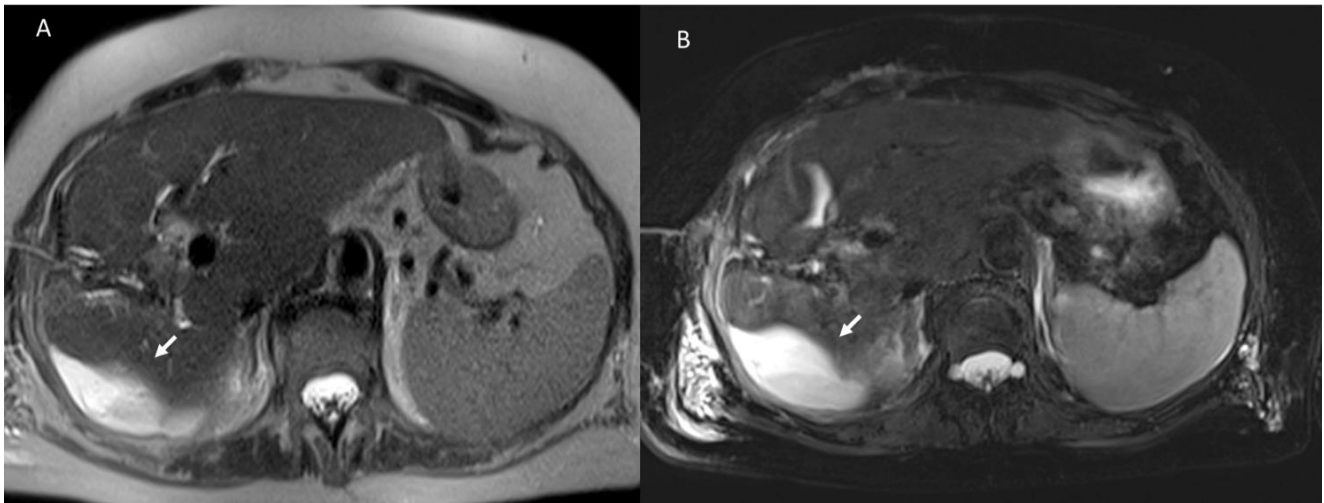


**Figure 1.** Postsurgical biloma assessed with MRI at 1 week post resection of VIII segment for liver metastasis. The biloma (arrow) appears hyperintense in T2 (A,B) sequences of MRI study.

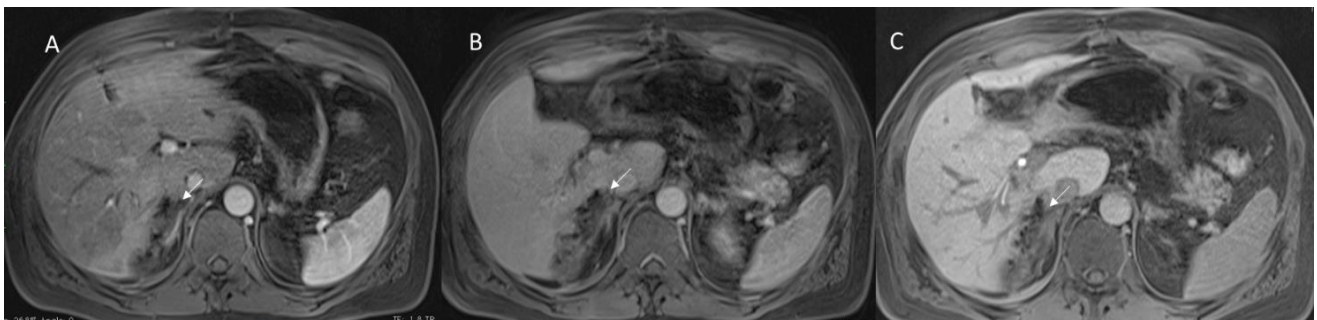


**Figure 2.** Hepatic abscess in resected cholangiocarcinoma on VI hepatic segment, evaluated with MRI. Arrow shows air artifacts within the collection and hyperenhancement of hepatic parenchymal in arterial phase (A) of contrast study that disappears in portal (B) and hepatobiliary (C) phase of contrast study.

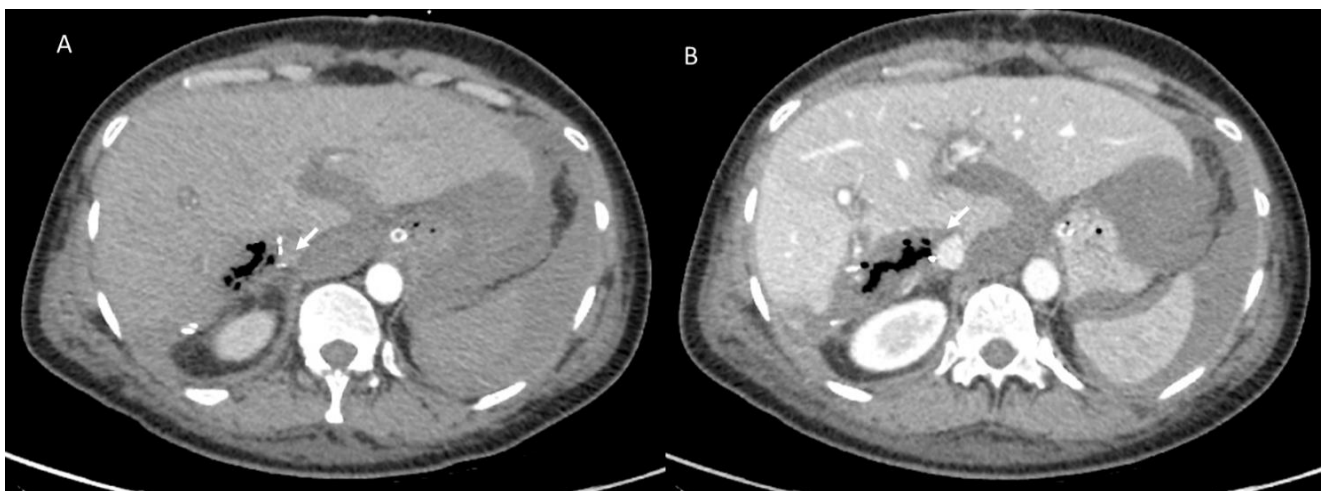


**Figure 3.** Hepatic abscess in resected hepatocellular carcinoma on VI hepatic segment, evaluated with CT. Arrow shows air artifacts within the collection in arterial (A) and portal (B) phase of contrast study.



Biloma could be defined as an encapsulated store of bile outside the biliary tree and within the abdominal cavity [116]. It is more homogeneous than hematomas, with density values much closer to that of water [116]. On US, bilomas appear as simple cyst-like collections, compared to the greater echogenicity of hematomas. In the case of overinfection, the mass tends to appear more structured with a mixed content of cellular debris and bile [115].

The presence of air artifacts detected within the collection and the absence of central perfusion on color Doppler examination in patients with fever and a decline in physical conditions suggest an abscess formation [115]. CT usually confirms the diagnosis with the typical findings of a central hypodense core of fluid material surrounded by a hyperdense rim and a hypodense outer ring as a double target appearance [115]. Percutaneous drainage should be considered in the case of infected collections (abscesses and bilomas) (Figure 4) [117–119], when a worsening of laboratory and clinical parameters occurs despite antibiotic therapy.

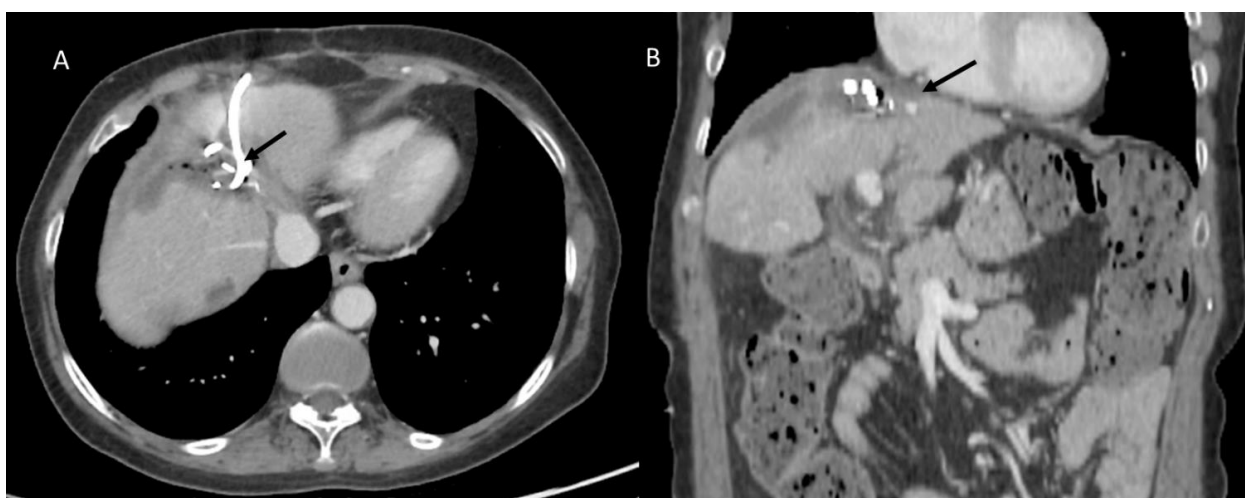


**Figure 4.** CT-guided hepatic infected biloma drainage (arrows) and postprocedure assessment in portal phase of contrast study in axial (A) and coronal (B) plane.

US is the first-level imaging method in the study of fluid collection, allowing for the definition of the location, dimension, and composition of the lesion, and it could guide the possible drainage. CECT should be performed in doubtful cases. Thanks to its spatial resolution and the possibility to conduct multiplanar reconstructions (MPR), CT allows to evaluate not only complex collections defining boundaries with adjacent structures, but also to reveal possible associated complications [115]. A multiphase CT protocol should comprise an unenhanced phase that easily detects one hematoma store, an arterial phase to intercept any source of bleeding, and a portal phase that allows to identify hepatic abscesses [115,120–122].

### 3.1.2. Posthepatectomy Hemorrhage

Posthepatectomy hemorrhage (PHH) is a major complication, which can substantially increase morbidity and mortality rates, with a described incidence of 1–8% [123]. In recent years, the International Study Group of Liver Surgery (ISGLS) has suggested a novel definition and staging of PHH with the aim of obtaining a standardized report of complications [124]. According to these guidelines, PHH is defined as a decrease in hemoglobin level  $>3$  g/dL compared to the postoperative baseline level (i.e., hemoglobin level immediately after surgery) and has three grades of severity (A–B–C), depending on the therapeutic strategy needed. In particular, a grade A hemorrhage could be controlled with minimal transfusion, while a grade B may need up to two transfusions in combination with medical anticoagulation therapy and/or the administration of procoagulant agents. Finally,

grade C corresponds to a life-threatening situation that requires radiological interventional treatment (such as embolization) or open surgery to manage the bleeding [124].

Currently, the known bleeding causes are: (a) bleeding from the surfaces of the remnant liver for arterial branch section or congestion of the hepatic vein due to stenosis or ligation; (b) partial or incomplete intraoperative hemostasis due to an improper manipulation of the hepatic vein root or trauma to the diaphragm; and (c) vascular sutures that could result in a slackening or falling off, an event which usually is due to elevated pressure in the vena cava from patient body movement, such as rolling or coughing intensely [124]. The suspicion of a hemorrhage arises from worsening clinical and laboratory parameters and the presence of blood loss from the abdominal drains [124].

The US findings should be nonspecific, consisting of a detection of intraabdominal fluid that may be iso-ipo or hyperechogenic or, in selected cases, in color Doppler identification, of turbulent flow at the possible bleeding site [115]. In order to obtain a definite diagnosis of PHH and eliminate other potential causes of bleeding, a multiphase CT study is mandatory [125]. On baseline examination, a blood collection with a superfluid attenuation of 30–45 HU could be found caudally from the perihepatic space along the right paracolic gutter up to the rectouterine or retro bladder space [125]. A strategy that can help in recognizing the bleeding site is to look for the sentinel clot sign, which is the closest to the origin of bleeding with attenuation values of 45–70 HU [126]. During the arterial phase, the active overflow of contrast material (Figure 5) with a mean attenuation value of 132 HU is evocative of arterial bleeding, which could assume three main morphologic patterns: a focal, spotted, or jet-like appearance [127,128]. The venous phase is certainly diriment in all those cases of low-flow bleeding [128].

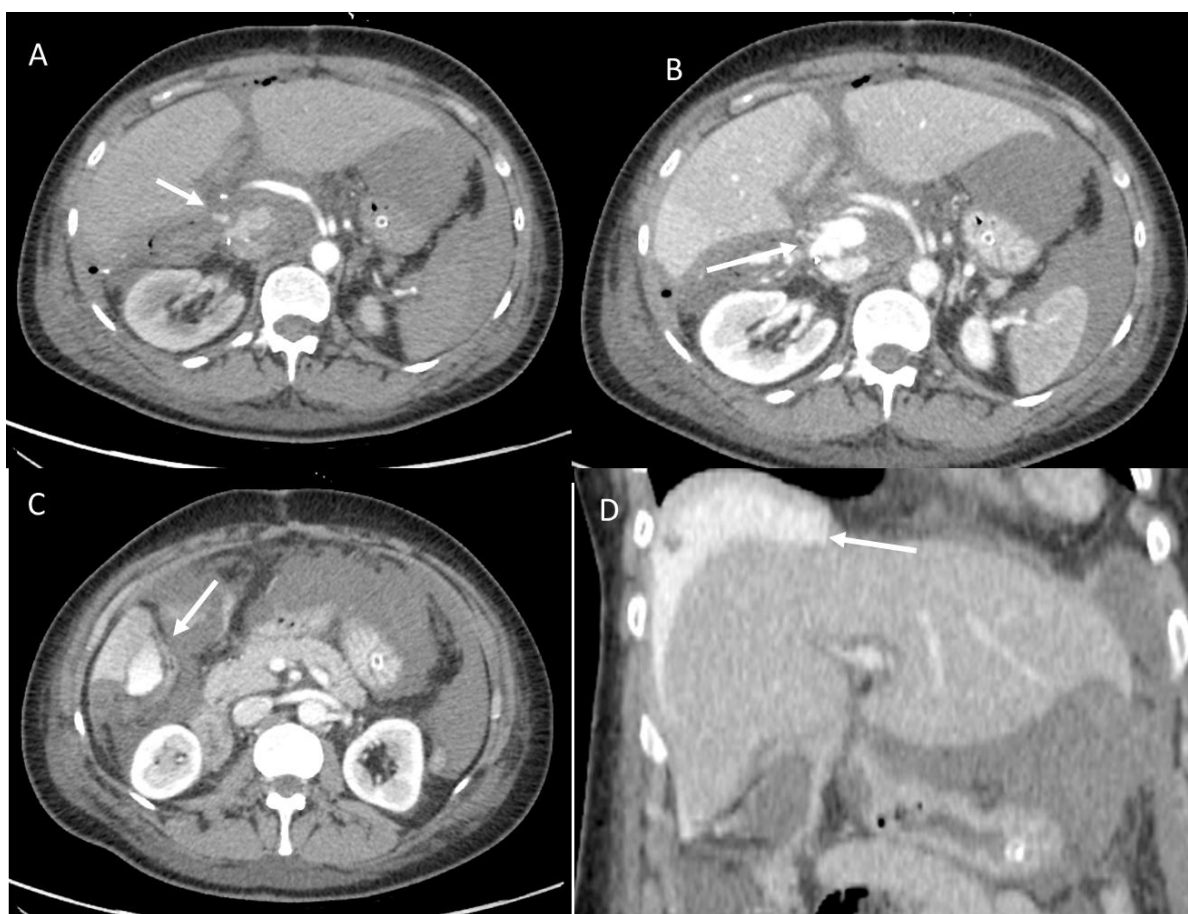


**Figure 5.** Active bleeding (arrow) during arterial (A), portal (B), and late (C) phase of contrast study. In (D), arrow shows contrast collection in perihepatic space.

### 3.1.3. Vascular Thrombosis

Postoperative vascular thrombosis is an uncommon complication, which could affect the hepatic and portal branches (Figure 6). A decline in liver function during the early postoperative days is highly indicative of a possible vascular thrombosis. The most frequent event after liver resection is a partial rather than complete hepatic vein occlusion next to resection margins. Although rare, acute Budd–Chiari syndrome (ABCS) may occur after liver resection, with a potentially lethal outcome. Di Domenico et al. described the development of ABCS after an extended right hepatectomy as being due to a contortion of the inferior vena cava or a twist of the left hepatic vein on the remaining liver with an outflow obstruction [129]. The rate of portal vein thrombosis (PVT) is low (about 3%); frequently, a segmental branch is involved (6%) [130]. Clinically, PVT may be undetected because of the absence of specific symptoms. Patients may report abdominal pain if it involves the superior mesenteric vessels and develop bowel congestion or ischemia. In addition, patients could report nausea, vomiting, anorexia, weight loss, diarrhea, or increased abdominal swelling secondary to ascites [131,132]. If acute thrombosis is not identified, collateral vessels will expand, and the patient will advance to cavernous transformation of the portal vein and portal hypertension, which may be evident as varices, splenomegaly, and hemorrhaging [133].

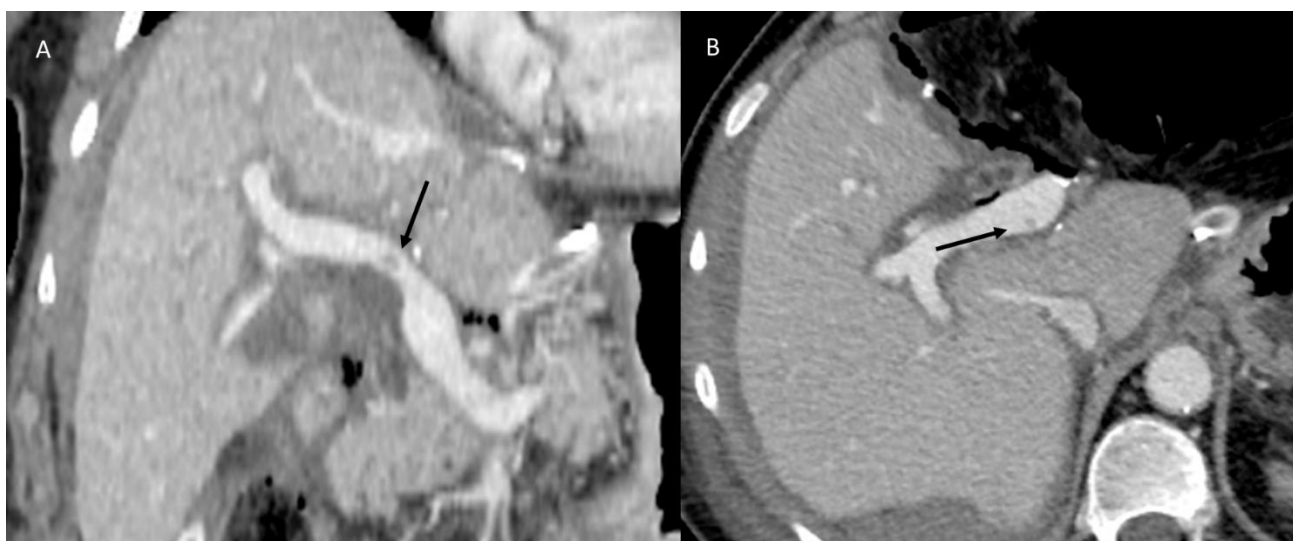


**Figure 6.** CT portal phase assessment in resected liver metastases patient. The arrow shows (A,B) mild portal thrombosis.

Even rarer is the possibility of arterial thrombosis (HAT), which generally occurs in association with vascular resection and microsurgical reconstruction during the treatment of advanced malignancies [134]. Clinically, HAT can present severely with graft failure (in the case of onset after liver transplant), sepsis, or abscess. In addition, it may present as cholangitis, bile leaks, or modified liver function tests [135,136]. US is a valuable examination tool in suspected vascular thrombosis. A circumscribed thrombus appears as an echogenic area within the affected vessel, with a complete lack or with a slow portal flow in the case of portal vein thrombosis on Doppler images. Color Doppler US is the more appropriate instrument to investigate an ABCS, identified by a loss of triphasic waveforms pattern with a radical decrease in hepatic vein velocity and simultaneous decrease in portal flow, in some cases becoming hepatofugal [137,138]. On the CECT image, during the arterial phase, an intraluminal filling defect referable to a thrombus of the hepatic artery could be easily detected. Venous thrombosis could be intercepted on an unenhanced CT scan as intraluminal hyperattenuating spots within the vessel [115]. Generally, these findings could be associated with a segmental enhancement of the tributary liver parenchyma,

paradoxically of increased attenuation due to a compensatory augmentation of the local arterial flow [115].

#### 3.1.4. Biliary Injuries

The most frequent postoperative biliary complications are bile leaks (Figure 7), occurring in 5% of cases after liver resection. The ISGLS has suggested a standardized definition of a bile leak, described as a bilirubin level in a drain three times the serum concentration on or after three postoperative days or the necessity of radiologic or operative intervention from a biliary store or bile peritonitis [139]. The leakage can arise from an incompetent bile-digestive anastomosis or from direct damage to the bile ducts during a surgical procedure or removal of a drainage tube [140,141]. If not promptly recognized, a bile leak may lead to sepsis and liver failure with an increased mortality rate [142].

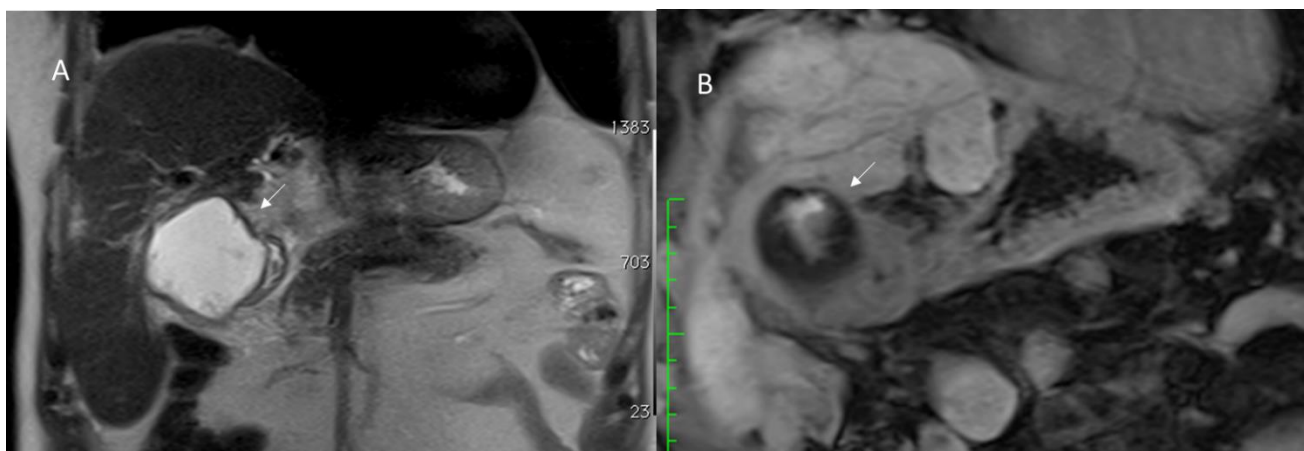


**Figure 7.** Bile leaks assessed with MRI T2-W sequence (A) and hepatospecific phase of contrast study (B). Arrow shows leak.

Nagano et al. proposed a classification of postoperative bile leaks after liver surgery in four categories (A-B-C-D), depending on the caliber and site of the injured ductal wall. Specifically, type A identifies self-limiting minor leaks from small bile ducts on the surface of the liver. Type B includes leaks from the main bile duct branches on the liver surface, while type C comprises main duct injuries close to the hepatic hilum. Finally, type D leakage matches with a total transected duct, without any connection with the main duct [143].

Direct opacification of the bile ducts through the surgical drainage could be appropriate rather than US examination or a CT scan, which could only detect nonspecific collection near the resection margins. Magnetic resonance cholangiopancreatography (MRCP) using gadolinium-based hepatobiliary contrast agents is the gold standard to distinguish the site and the type of the leakage, with a high diagnostic accuracy [144,145].

Invasive diagnostic modalities to define biliary leaks include endoscopic retrograde cholangiopancreatography (ERCP) that allows for the therapeutic management such as the placement of biliary stents and Percutaneous Transhepatic Cholangiography (PTC). ERCP is characterized by some limitations that include the inability to assess the proximal tract of the biliary tree and a difficult passage of the endoscope in postsurgical biliary–enteric anastomosis [146,147]. In the case of postsurgical bile duct damage, interventional radiological treatment includes percutaneous drainage of fluid collections, characterization of the biliary tract anatomy and evaluation of the site and the extent of bile duct injury with PTC, and biliary diversion from the site of bile leakage with external biliary drainage. Percutaneous interventional procedures can arise from definitive treatment or temporization prior to definitive surgical repair that is necessary only in few cases [147,148].

Although extremely rare, an intraoperative diaphragmatic injury may occur, especially during treatment of masses on the right liver. Diaphragmatic injuries generally are



self-limiting conditions, but they could be associated with bowel herniation and subsequent perforation. These complications could be hard to classify clinically due to frequent postoperative ileus by aesthetic drugs. CT is often required for a conclusive diagnosis. A diaphragmatic disruption may also lead to biliary fistulae. In this circumstance, CT may show a right pleural diffusion with higher pleural enhancement or a direct passage of a contrast medium agent through the fistulous path [149].

### 3.2. Late Postoperative Complications

#### 3.2.1. Disease Recurrence

Multiphasic CT and MR imaging could be employed in the investigation of disease recurrence.

Gadoxetic acid-enhanced MR imaging is more sensitive than MDCT for discovering the intrahepatic recurrence of HCC after hepatic surgery (98.1% and 67.2%, respectively), with similar specificity values (85% and 90%, respectively) [150].

The CT protocol in postsurgical follow-up varies according to the type of primary resected hepatic tumor. While a baseline scan is unnecessary in most cases, an acquisition during the arterial phase is essential in the evaluation of recurrences from HCC and neuroendocrine tumors [151–153] before a portal venous phase. Pre- and postcontrast sequences are mandatory for MRI studies. The detection of biliary dilatation even if there is no obvious mass may always increase the suspicion of recurrence [154–157].

The rate of recurrence after 5 years from hepatic resection of HCC ranges from 50 to 70% [158,159]. Approximately half of surgically treated cholangiocarcinoma, particularly intrahepatic type, relapse within 5 years after treatment [160]. CT and MRI, including MRCP sequences, are the modalities of choice in the follow-up of these patients, in some cases supplemented by 18FDG positron emission tomography (PET)/CT investigations that can recognize early disease recurrence [161].

The recurrence rate in patients treated surgically for liver metastases is about 60%, with a particularly high frequency of liver recurrence (40%) [162]. The risk of tumor regrowth along the resection margins is increased if a metastasectomy rather than a segmental resection is performed, due to a higher chance of positive margins [163]. Integrated preoperative planning using hepatospecific contrast-enhanced MRI and CECT is essential to map secondary injuries and assess their link with vascular and biliary structures. In addition, in the postsurgical follow-up, CT, especially the portal phase (Figure 8) and MRI with diffusion and contrast-enhanced sequences, are the methods of choice in identifying disease relapse [150].

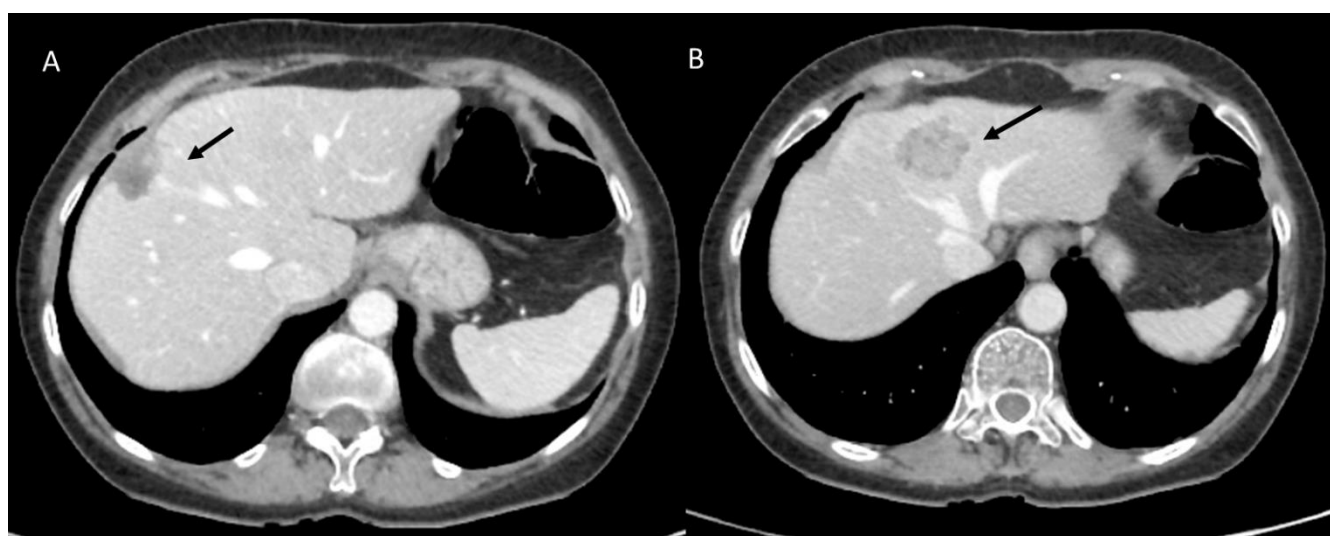


**Figure 8.** CT assessment in colorectal metastasis-resected patient (A). In (B), arrow shows a new lesion.

### 3.2.2. Late Strictures and Ischemic Cholangitis

Biliary strictures (Figure 9) are the most frequent late complications, usually developing anywhere from a few months to many years after surgery [164]. A bile duct is stenotic if the lumen is found sufficiently reduced to justify blood chemistry alterations and impaired bile flow, resulting in obstructive jaundice and liver dysfunction. Despite the reduced caliber, radiological characteristics that may be suggestive of a biliary stricture involve intra- and extrahepatic bile duct dilatation (a diameter of more than 3 or 8 mm, respectively), ductal narrowing, and incomplete display of part of the duct [165]. The most common strictures are the anastomotic type, usually determined by iatrogenic bile duct injury, resulting in bile leakage and scar formation [165].

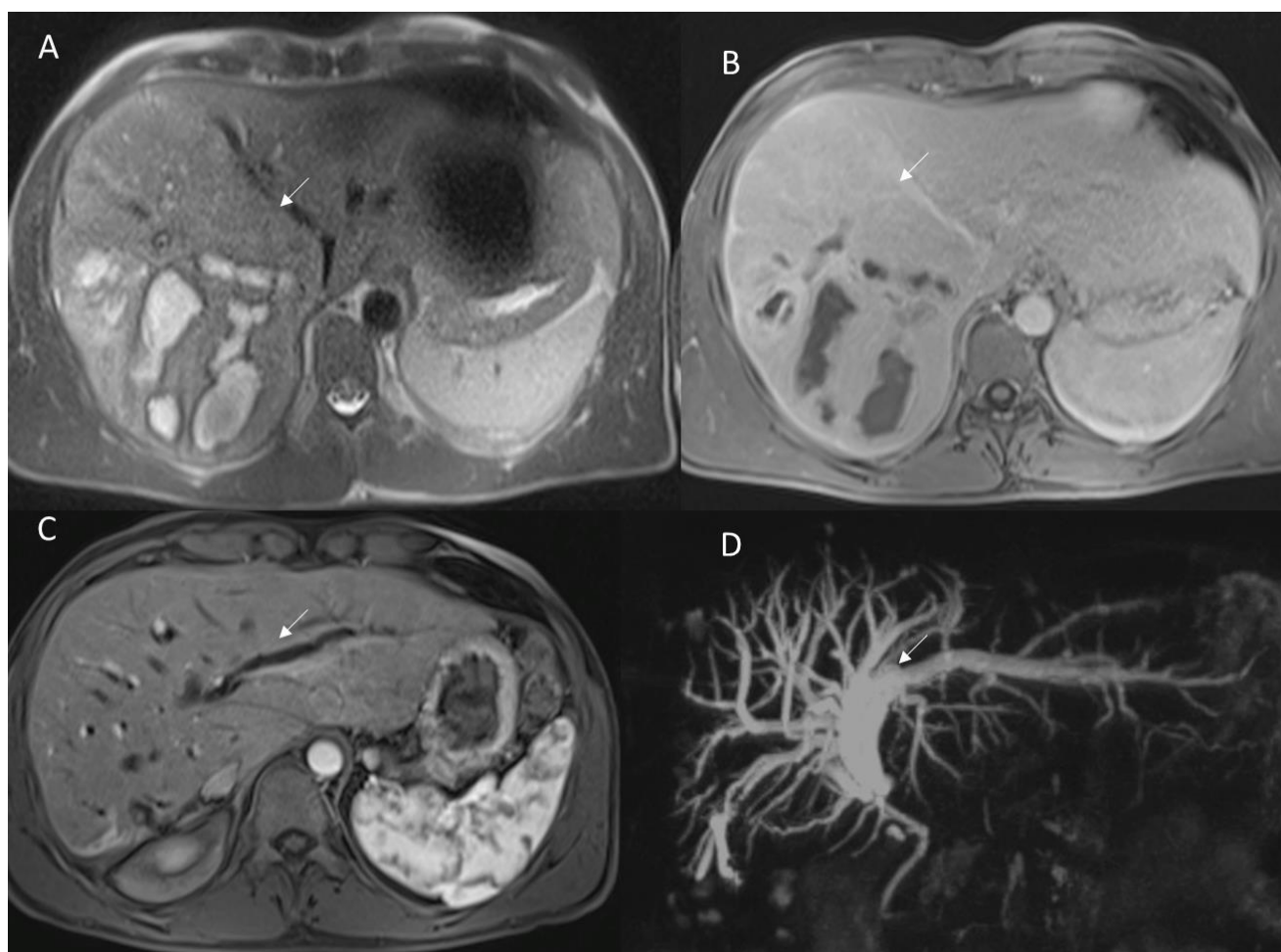


**Figure 9.** Patient with hepatosarcoma evaluated with MRI study ((A): T2-W sequence and (B): portal phase of contrast study). At MRI 6-month evaluation of arterial phase (C) and cholangiography (D) sequences show biliary strictures (arrow).

On CT examination, a dilated fluid-filled Roux-en-Y loop with an upstream dilatation of the biliary tree could be observed, with a fat stranding sign close to the treated area. MRCP is particularly helpful in these kinds of lesions, since the endoscopic approach is only possible in rare cases, and percutaneous transhepatic cholangiography may be related to an increased risk of complications [164]. On MRI images, the obstruction should be considered complete if the morphology of the anastomosis is altered with an empty signal between the ducts and a fluid-filled jejunal loop, in the presence of intrahepatic biliary duct enlargement [164].

Another type of stricture is the non-anastomotic one, of which ischaemic cholangitis is the most frequent cause. An ischaemic injury resulting from thrombosis of the hepatic

artery is the pathophysiological basis for the formation of this type of stenosis. Although, ischaemic cholangitis is a disorder that could occur after orthotopic liver transplantation, it has occurred after liver resection. MRCP is the gold standard technique in the diagnosis of nonanastomotic biliary strictures. The classic picture is that of long ductal segmental hilar stenosis that includes the right and left hepatic ducts and the biliary confluence, connected with the dilatation of the intrahepatic bile tree [141,165].

#### 4. Multidisciplinary Assessment

The management after a hepatectomy requires a multidisciplinary treatment, which involves surgeons, interventional radiologists, and gastroenterologists. Although several complications are self-limiting and do not require treatment, when the patient's life is at risk, it would be appropriate to consider the possibility of a minimally invasive intervention to reduce the risk of further complications in an already critical patient. Therefore, the collaboration of the interventional radiologist and the surgeon should be consistent [166–170]. In addition, a dedicated and expert radiologist would be crucial to identify all critical conditions as soon as possible

#### 5. Conclusions

The increase in surgical procedures on the liver has concurrently increased the number of postoperative complications. Elderly patients with significant comorbidities, extended resections, iterative surgeries, and previous chemotherapy are all risk factors for the onset of postoperative complications.

Radiology plays an important role in the early discovery of complications, sometimes with the use of invasive diagnostic modalities, such as ERCP, in their treatment.

Whereas ultrasonography is often the first-line imaging investigation when a postoperative complication is suspected, CT is of greater value for identifying early postoperative pathologic fluid collection, bleeding, and vascular thrombosis, while MRCP is the imaging modality of choice for the characterization of early postoperative bile duct injuries.

MDCT and MR imaging could also be useful in the identification of disease recurrence. Lastly, MRCP also produces the diagnosis of late ischemic cholangitis that may happen after intraoperative arterial injury.

A correct description of these disorders will allow a timely diagnosis and specific management of potentially life-threatening postoperative complications.

**Funding:** This research received no external funding.

**Institutional Review Board Statement:** Not applicable.

**Informed Consent Statement:** Not applicable.

**Data Availability Statement:** Data are available at link <https://zenodo.org/record/6579378#.Yo8zCahBy3A> (accessed on 8 May 2022).

**Acknowledgments:** The authors are grateful to Alessandra Trocino, librarian at the National Cancer Institute of Naples, Italy. Moreover, for their collaboration, the authors are grateful for the research support of Paolo Pariante, Martina Totaro and Andrea Esposito of Radiology Division, "Istituto Nazionale Tumori IRCCS Fondazione Pascale—IRCCS di Napoli", Naples, I-80131, Italy.

**Conflicts of Interest:** The authors have no conflict of interest to disclose. The authors confirm that the article is not under consideration for publication elsewhere.

#### References

1. Lafaro, K.J.; Stewart, C.; Fong, A.; Fong, Y. Robotic Liver Resection. *Surg. Clin. N. Am.* **2020**, *100*, 265–281. [CrossRef] [PubMed]
2. Agarwal, V.; Divatia, J.V. Enhanced recovery after surgery in liver resection: Current concepts and controversies. *Korean J. Anesthesiol.* **2019**, *72*, 119–129. [CrossRef] [PubMed]
3. Izzo, F.; Granata, V.; Grassi, R.; Fusco, R.; Palaia, R.; Delrio, P.; Carrafiello, G.; Azoulay, D.; Petrillo, A.; Curley, S.A. Radiofrequency Ablation and Microwave Ablation in Liver Tumors: An Update. *Oncologist* **2019**, *24*, e990–e1005. [CrossRef] [PubMed]

4. Granata, V.; Grassi, R.; Fusco, R.; Setola, S.V.; Belli, A.; Ottaiano, A.; Nasti, G.; La Porta, M.; Danti, G.; Cappabianca, S.; et al. Intrahepatic cholangiocarcinoma and its differential diagnosis at MRI: How radiologist should assess MR features. *Radiol. Med.* **2021**, *126*, 1584–1600. [[CrossRef](#)]
5. Hussein, M.A.M.; Cafarelli, F.P.; Paparella, M.T.; Rennie, W.J.; Guglielmi, G. Phosphaturic mesenchymal tumors: Radiological aspects and suggested imaging pathway. *Radiol. Med.* **2021**, *126*, 1609–1618. [[CrossRef](#)]
6. Granata, V.; Fusco, R.; Avallone, A.; Catalano, O.; Piccirillo, M.; Palaia, R.; Nasti, G.; Petrillo, A.; Izzo, F. A radiologist's point of view in the presurgical and intraoperative setting of colorectal liver metastases. *Future Oncol.* **2018**, *14*, 2189–2206. [[CrossRef](#)]
7. Fanelli, F.; Cannavale, A.; Chisci, E.; Citone, M.; Falcone, G.M.; Michelagnoli, S.; Miele, V. Direct percutaneous embolization of aneurysm sac: A safe and effective procedure to treat post-EVAR type II endoleaks. *Radiol. Med.* **2021**, *126*, 258–263. [[CrossRef](#)]
8. Granata, V.; Fusco, R.; Catalano, O.; Piccirillo, M.; De Bellis, M.; Izzo, F.; Petrillo, A. Percutaneous ablation therapy of hepatocellular carcinoma with irreversible electroporation: MRI findings. *AJR Am. J. Roentgenol.* **2015**, *204*, 1000–1007. [[CrossRef](#)]
9. Granata, V.; Fusco, R.; Catalano, O.; Avallone, A.; Palaia, R.; Botti, G.; Tatangelo, F.; Granata, F.; Cascella, M.; Izzo, F.; et al. Diagnostic accuracy of magnetic resonance, computed tomography and contrast enhanced ultrasound in radiological multimodality assessment of peribiliary liver metastases. *PLoS ONE* **2017**, *12*, e0179951. [[CrossRef](#)]
10. Dimick, J.B.; Wainess, R.M.; Cowan, J.A.; Upchurch, G.R.; Knol, J.A.; Colletti, L.M. National trends in the use and outcomes of hepatic resection. *J. Am. Coll. Surg.* **2004**, *199*, 31–38. [[CrossRef](#)]
11. Giurazza, F.; Contegiacomo, A.; Calandri, M.; Mosconi, C.; Modestino, F.; Corvino, F.; Scrofani, A.R.; Marra, P.; Coniglio, G.; Failla, G.; et al. IVC filter retrieval: A multicenter proposal of two score systems to predict application of complex technique and procedural outcome. *Radiol. Med.* **2021**, *126*, 1007–1016. [[CrossRef](#)] [[PubMed](#)]
12. Asiyanbola, B.; Chang, D.; Gleisner, A.L.; Nathan, H.; Choti, M.A.; Schulick, R.D.; Pawlik, T.M. Operative mortality after hepatic resection: Are literature-based rates broadly applicable? *J. Gastrointest. Surg.* **2008**, *12*, 842–851. [[CrossRef](#)] [[PubMed](#)]
13. Mullen, J.T.; Ribero, D.; Reddy, S.K.; Donadon, M.; Zorzi, D.; Gautam, S.; Abdalla, E.K.; Curley, S.A.; Capussotti, L.; Clary, B.M.; et al. Hepatic insufficiency and mortality in 1059 noncirrhotic patients undergoing major hepatectomy. *J. Am. Coll. Surg.* **2007**, *204*, 854–862. [[CrossRef](#)]
14. Barabino, M.; Gurgitano, M.; Fochesato, C.; Angileri, S.A.; Franceschelli, G.; Santambrogio, R.; Mariani, N.M.; Opocher, E.; Carrafiello, G. LI-RADS to categorize liver nodules in patients at risk of HCC: Tool or a gadget in daily practice? *Radiol. Med.* **2021**, *126*, 5–13. [[CrossRef](#)] [[PubMed](#)]
15. Mathur, A.K.; Ghaferi, A.A.; Osborne, N.H.; Pawlik, T.M.; Campbell, D.A.; Englesbe, M.J.; Welling, T.H. Body mass index and adverse perioperative outcomes following hepatic resection. *J. Gastrointest. Surg.* **2010**, *14*, 1285–1291. [[CrossRef](#)] [[PubMed](#)]
16. Benzoni, E.; Cojutti, A.; Lorenzin, D.; Adani, G.L.; Baccarani, U.; Favero, A.; Zompicchiati, A.; Bresadola, F.; Uzzau, A. Liver resective surgery: A multivariate analysis of postoperative outcome and complication. *Langenbecks Arch. Surg.* **2007**, *392*, 45–54. [[CrossRef](#)]
17. Sadamori, H.; Yagi, T.; Shinoura, S.; Umeda, Y.; Yoshida, R.; Satoh, D.; Nobuoka, D.; Utsumi, M.; Fujiwara, T. Risk factors for major morbidity after liver resection for hepatocellular carcinoma. *Br. J. Surg.* **2013**, *100*, 122–129. [[CrossRef](#)]
18. Granata, V.; Fusco, R.; Venanzio Setola, S.; Mattace Raso, M.; Avallone, A.; De Stefano, A.; Nasti, G.; Palaia, R.; Delrio, P.; Petrillo, A.; et al. Liver radiologic findings of chemotherapy-induced toxicity in liver colorectal metastases patients. *Eur. Rev. Med. Pharmacol. Sci.* **2019**, *23*, 9697–9706. [[CrossRef](#)]
19. Avallone, A.; Pecori, B.; Bianco, F.; Aloj, L.; Tatangelo, F.; Romano, C.; Granata, V.; Marone, P.; Leone, A.; Botti, G.; et al. Critical role of bevacizumab scheduling in combination with pre-surgical chemo-radiotherapy in MRI-defined high-risk locally advanced rectal cancer: Results of the BRANCH trial. *Oncotarget* **2015**, *6*, 30394–30407. [[CrossRef](#)]
20. Hu, H.T.; Shan, Q.Y.; Chen, S.L.; Li, B.; Feng, S.T.; Xu, E.J.; Li, X.; Long, J.Y.; Xie, X.Y.; Lu, M.D.; et al. CT-based radiomics for preoperative prediction of early recurrent hepatocellular carcinoma: Technical reproducibility of acquisition and scanners. *Radiol. Med.* **2020**, *125*, 697–705. [[CrossRef](#)]
21. Gabelloni, M.; Di Nasso, M.; Morganti, R.; Faggioni, L.; Masi, G.; Falcone, A.; Neri, E. Application of the ESR iGuide clinical decision support system to the imaging pathway of patients with hepatocellular carcinoma and cholangiocarcinoma: Preliminary findings. *Radiol. Med.* **2020**, *125*, 531–537. [[CrossRef](#)] [[PubMed](#)]
22. Gatti, M.; Calandri, M.; Bergamasco, L.; Darvizeh, F.; Grazioli, L.; Inchingolo, R.; Ippolito, D.; Rousset, S.; Veltri, A.; Fonio, P.; et al. Characterization of the arterial enhancement pattern of focal liver lesions by multiple arterial phase magnetic resonance imaging: Comparison between hepatocellular carcinoma and focal nodular hyperplasia. *Radiol. Med.* **2020**, *125*, 348–355. [[CrossRef](#)] [[PubMed](#)]
23. Granata, V.; Fusco, R.; de Lutio di Castelguidone, E.; Avallone, A.; Palaia, R.; Delrio, P.; Tatangelo, F.; Botti, G.; Grassi, R.; Izzo, F.; et al. Diagnostic performance of gadoteric acid-enhanced liver MRI versus multidetector CT in the assessment of colorectal liver metastases compared to hepatic resection. *BMC Gastroenterol.* **2019**, *19*, 129. [[CrossRef](#)] [[PubMed](#)]
24. Agostini, A.; Borgheresi, A.; Mari, A.; Floridi, C.; Bruno, F.; Carotti, M.; Schicchi, N.; Barile, A.; Maggi, S.; Giovagnoni, A. Dual-energy CT: Theoretical principles and clinical applications. *Radiol. Med.* **2019**, *124*, 1281–1295. [[CrossRef](#)] [[PubMed](#)]
25. Bertocchi, E.; Barugola, G.; Nicosia, L.; Mazzola, R.; Ricchetti, F.; Dell'Abate, P.; Alongi, F.; Ruffo, G. A comparative analysis between radiation dose intensification and conventional fractionation in neoadjuvant locally advanced rectal cancer: A monocentric prospective observational study. *Radiol. Med.* **2020**, *125*, 990–998. [[CrossRef](#)]



26. Agostini, A.; Floridi, C.; Borgheresi, A.; Badaloni, M.; Esposito Pirani, P.; Terilli, F.; Ottaviani, L.; Giovagnoni, A. Proposal of a low-dose, long-pitch, dual-source chest CT protocol on third-generation dual-source CT using a tin filter for spectral shaping at 100 kVp for CoronaVirus Disease 2019 (COVID-19) patients: A feasibility study. *Radiol. Med.* **2020**, *125*, 365–373. [[CrossRef](#)]
27. Cicero, G.; Ascenti, G.; Albrecht, M.H.; Blandino, A.; Cavallaro, M.; D'Angelo, T.; Carerj, M.L.; Vogl, T.J.; Mazziotti, S. Extra-abdominal dual-energy CT applications: A comprehensive overview. *Radiol. Med.* **2020**, *125*, 384–397. [[CrossRef](#)]
28. Bottari, A.; Silipigni, S.; Carerj, M.L.; Cattafi, A.; Maimone, S.; Marino, M.A.; Mazziotti, S.; Pitrone, A.; Squadrito, G.; Ascenti, G. Dual-source dual-energy CT in the evaluation of hepatic fractional extracellular space in cirrhosis. *Radiol. Med.* **2020**, *125*, 7–14. [[CrossRef](#)]
29. Cicero, G.; Mazziotti, S.; Silipigni, S.; Blandino, A.; Cantisani, V.; Pergolizzi, S.; D'Angelo, T.; Stagno, A.; Maimone, S.; Squadrito, G.; et al. Dual-energy CT quantification of fractional extracellular space in cirrhotic patients: Comparison between early and delayed equilibrium phases and correlation with oesophageal varices. *Radiol. Med.* **2021**, *126*, 761–767. [[CrossRef](#)]
30. Cereser, L.; Girometti, R.; Da Re, J.; Marchesini, F.; Como, G.; Zuiani, C. Inter-reader agreement of high-resolution computed tomography findings in patients with COVID-19 pneumonia: A multi-reader study. *Radiol. Med.* **2021**, *126*, 577–584. [[CrossRef](#)]
31. Granata, V.; Fusco, R.; Setola, S.V.; De Muzio, F.; Dell' Aversana, F.; Cutolo, C.; Faggioni, L.; Miele, V.; Izzo, F.; Petrillo, A. CT-Based Radiomics Analysis to Predict Histopathological Outcomes Following Liver Resection in Colorectal Liver Metastases. *Cancers* **2022**, *14*, 1648. [[CrossRef](#)] [[PubMed](#)]
32. Granata, V.; Fusco, R.; Costa, M.; Picone, C.; Cozzi, D.; Moroni, C.; La Casella, G.V.; Montanino, A.; Monti, R.; Mazzoni, F.; et al. Preliminary Report on Computed Tomography Radiomics Features as Biomarkers to Immunotherapy Selection in Lung Adenocarcinoma Patients. *Cancers* **2021**, *13*, 3992. [[CrossRef](#)] [[PubMed](#)]
33. Fiorentino, A.; Gregucci, F.; Bonaparte, I.; Vitulano, N.; Surgo, A.; Mazzola, R.; Di Monaco, A.; Carbonara, R.; Alongi, F.; Langialonga, T.; et al. Stereotactic Ablative radiation therapy (SABR) for cardiac arrhythmia: A new therapeutic option? *Radiol. Med.* **2021**, *126*, 155–162. [[CrossRef](#)] [[PubMed](#)]
34. Agostini, A.; Borgheresi, A.; Carotti, M.; Ottaviani, L.; Badaloni, M.; Floridi, C.; Giovagnoni, A. Third-generation iterative reconstruction on a dual-source, high-pitch, low-dose chest CT protocol with tin filter for spectral shaping at 100 kV: A study on a small series of COVID-19 patients. *Radiol. Med.* **2021**, *126*, 388–398. [[CrossRef](#)] [[PubMed](#)]
35. Granata, V.; Fusco, R.; De Muzio, F.; Cutolo, C.; Setola, S.V.; Grassi, R.; Grassi, F.; Ottaiano, A.; Nasti, G.; Tatangelo, F.; et al. Radiomics textural features by MR imaging to assess clinical outcomes following liver resection in colorectal liver metastases. *Radiol. Med.* **2022**, *127*, 461–470. [[CrossRef](#)] [[PubMed](#)]
36. Granata, V.; Fusco, R.; De Muzio, F.; Cutolo, C.; Setola, S.V.; Dell' Aversana, F.; Ottaiano, A.; Avallone, A.; Nasti, G.; Grassi, F.; et al. Contrast MR-Based Radiomics and Machine Learning Analysis to Assess Clinical Outcomes following Liver Resection in Colorectal Liver Metastases: A Preliminary Study. *Cancers* **2022**, *14*, 1110. [[CrossRef](#)]
37. Granata, V.; Fusco, R.; De Muzio, F.; Cutolo, C.; Setola, S.V.; Dell' Aversana, F.; Ottaiano, A.; Nasti, G.; Grassi, R.; Pilone, V.; et al. EOB-MR Based Radiomics Analysis to Assess Clinical Outcomes following Liver Resection in Colorectal Liver Metastases. *Cancers* **2022**, *14*, 1239. [[CrossRef](#)]
38. Compagnone, G.; Padovani, R.; D'Ercole, L.; Orlacchio, A.; Bernardi, G.; D'Avanzo, M.A.; Grande, S.; Palma, A.; Campanella, F.; Rosi, A. Provision of Italian diagnostic reference levels for diagnostic and interventional radiology. *Radiol. Med.* **2021**, *126*, 99–105. [[CrossRef](#)]
39. Granata, V.; Fusco, R.; Avallone, A.; De Stefano, A.; Ottaiano, A.; Sbordone, C.; Brunese, L.; Izzo, F.; Petrillo, A. Radiomics-Derived Data by Contrast Enhanced Magnetic Resonance in RAS Mutations Detection in Colorectal Liver Metastases. *Cancers* **2021**, *13*, 453. [[CrossRef](#)]
40. Esposito, A.; Buscarino, V.; Raciti, D.; Casiraghi, E.; Manini, M.; Biondetti, P.; Forzenigo, L. Characterization of liver nodules in patients with chronic liver disease by MRI: Performance of the Liver Imaging Reporting and Data System (LI-RADS v.2018) scale and its comparison with the Likert scale. *Radiol. Med.* **2020**, *125*, 15–23. [[CrossRef](#)]
41. Orsatti, G.; Zucchetta, P.; Varotto, A.; Crimi, F.; Weber, M.; Cecchin, D.; Bisogno, G.; Spimpolo, A.; Giraudo, C.; Stramare, R. Volumetric histograms-based analysis of apparent diffusion coefficients and standard uptake values for the assessment of pediatric sarcoma at staging: Preliminary results of a PET/MRI study. *Radiol. Med.* **2021**, *126*, 878–885. [[CrossRef](#)] [[PubMed](#)]
42. Granata, V.; Fusco, R.; Catalano, O.; Setola, S.V.; de Lutio di Castelguidone, E.; Piccirillo, M.; Palaia, R.; Grassi, R.; Granata, F.; Izzo, F.; et al. Multidetector computer tomography in the pancreatic adenocarcinoma assessment: An update. *Infect Agent Cancer* **2016**, *11*, 57. [[CrossRef](#)] [[PubMed](#)]
43. Berardo, S.; Sukhovei, L.; Andorno, S.; Carriero, A.; Stecco, A. Quantitative bone marrow magnetic resonance imaging through apparent diffusion coefficient and fat fraction in multiple myeloma patients. *Radiol. Med.* **2021**, *126*, 445–452. [[CrossRef](#)] [[PubMed](#)]
44. Crimi, F.; Capelli, G.; Spolverato, G.; Bao, Q.R.; Florio, A.; Milite Rossi, S.; Cecchin, D.; Albertoni, L.; Campi, C.; Pucciarelli, S.; et al. MRI T2-weighted sequences-based texture analysis (TA) as a predictor of response to neoadjuvant chemo-radiotherapy (nCRT) in patients with locally advanced rectal cancer (LARC). *Radiol. Med.* **2020**, *125*, 1216–1224. [[CrossRef](#)] [[PubMed](#)]
45. Granata, V.; Fusco, R.; Sansone, M.; Grassi, R.; Maio, F.; Palaia, R.; Tatangelo, F.; Botti, G.; Grimm, R.; Curley, S.; et al. Magnetic resonance imaging in the assessment of pancreatic cancer with quantitative parameter extraction by means of dynamic contrast-enhanced magnetic resonance imaging, diffusion kurtosis imaging and intravoxel incoherent motion diffusion-weighted imaging. *Therap. Adv. Gastroenterol.* **2020**, *13*, 1756284819885052. [[CrossRef](#)] [[PubMed](#)]

46. Mungai, F.; Verrone, G.B.; Bonasera, L.; Bicci, E.; Pietragalla, M.; Nardi, C.; Berti, V.; Mazzoni, L.N.; Miele, V. Imaging biomarkers in the diagnosis of salivary gland tumors: The value of lesion/parenchyma ratio of perfusion-MR pharmacokinetic parameters. *Radiol. Med.* **2021**, *126*, 1345–1355. [[CrossRef](#)]
47. Fusco, R.; Granata, V.; Sansone, M.; Rega, D.; Delrio, P.; Tatangelo, F.; Romano, C.; Avallone, A.; Pupo, D.; Giordano, M.; et al. Validation of the standardized index of shape tool to analyze DCE-MRI data in the assessment of neo-adjuvant therapy in locally advanced rectal cancer. *Radiol. Med.* **2021**, *126*, 1044–1054. [[CrossRef](#)]
48. Bordonaro, V.; Ciancarella, P.; Ciliberti, P.; Curione, D.; Napolitano, C.; Santangelo, T.P.; Natali, G.L.; Rollo, M.; Guccione, P.; Pasquini, L.; et al. Dynamic contrast-enhanced magnetic resonance lymphangiography in pediatric patients with central lymphatic system disorders. *Radiol. Med.* **2021**, *126*, 737–743. [[CrossRef](#)]
49. Quinn, S.F.; Bodne, D.J.; Clark, R.A.; Karl, R.C.; Nicosia, S.V. Upper abdomen: CT findings following partial hepatectomy. *Radiology* **1988**, *168*, 879–880. [[CrossRef](#)]
50. Wigham, A.; Alexander Grant, L. Radiologic assessment of hepatobiliary surgical complications. *Semin. Ultrasound CT MR* **2013**, *34*, 18–31. [[CrossRef](#)]
51. Romano, S.; Tortora, G.; Scaglione, M.; Lassandro, F.; Guidi, G.; Grassi, R.; Romano, L. MDCT imaging of post interventional liver: A pictorial essay. *Eur. J. Radiol.* **2005**, *53*, 425–432. [[CrossRef](#)] [[PubMed](#)]
52. Arrive, L.; Hricak, H.; Goldberg, H.I.; Thoeni, R.F.; Margulis, A.R. MR appearance of the liver after partial hepatectomy. *Am. J. Roentgenol.* **1989**, *152*, 1215–1220. [[CrossRef](#)] [[PubMed](#)]
53. Molina-Romero, F.X.; Palma-Zamora, E.; Morales-Soriano, R.; Rodríguez-Pino, J.C.; González-Argente, F.X.; Morón-Canis, J.M. Comparison of anatomical resection and non-anatomical resection in patients with hepatocellular carcinoma: Propensity score matching method. *Cir. Cir.* **2019**, *87*, 328–336. [[CrossRef](#)] [[PubMed](#)]
54. Alonso Casado, O.; González Moreno, S.; Encinas García, S.; Rojo Sebastián, A.; Olavarría Delgado, A. Marcaje de metástasis hepática antes de quimioterapia neoadyuvante para su posterior localización y resección mediante hepatectomía no anatómica [Hepatic metastasis marking before neoadjuvant chemotherapy for their subsequent location and resection using non-anatomical hepatectomy]. *Cir. Esp.* **2013**, *91*, 687–689. (In Spanish) [[CrossRef](#)]
55. Lupo, L.; Gallerani, A.; Aquilino, F.; Di Palma, G.; De Fazio, M.; Guglielmi, A.; Memeo, V. Resezione anatomica epatica con termoablazione a radiofrequenza nel trattamento dei tumori primitivi o secondari del fegato [Anatomical hepatic resection using radiofrequency thermoablation in the treatment of primary or secondary liver tumors]. *Tumori* **2003**, *89* (Suppl. 4), 105–106. (In Italian)
56. Lee, M.K.T.; Gao, F.; Strasberg, S.M. Perceived complexity of various liver resections: Results of a survey of experts with development of a complexity score and classification. *J. Am. Coll. Surg.* **2015**, *220*, 64–69. [[CrossRef](#)]
57. Terminology Committee of the International Hepato-Pancreato-Biliary Association. Terminology of liver anatomy and resections. *HPB* **2000**, *2*, 333–339.
58. Zimmitti, G.; Roses, R.E.; Andreou, A.; Shindoh, J.; Curley, S.A.; Aloia, T.A.; Vauthey, J.N. Greater complexity of liver surgery is not associated with an increased incidence of liver-related complications except for bile leak: An experience with 2628 consecutive resections. *J. Gastrointest. Surg.* **2013**, *17*, 57–64. [[CrossRef](#)]
59. Li, G.Z.; Speicher, P.J.; Lidsky, M.E.; Darrabie, M.D.; Scarborough, J.E.; White, R.R.; Turley, R.S.; Clary, B.M. Hepatic resection for hepatocellular carcinoma: Do contemporary morbidity and mortality rates demand a transition to ablation as first-line treatment? *J. Am. Coll. Surg.* **2014**, *218*, 827–834. [[CrossRef](#)]
60. Okuda, K. Hepatocellular carcinoma. *J. Hepatol.* **2000**, *32*, 225–237. [[CrossRef](#)]
61. Orcutt, S.T.; Anaya, D.A. Liver Resection and Surgical Strategies for Management of Primary Liver Cancer. *Cancer Control* **2018**, *25*, 1073274817744621. [[CrossRef](#)] [[PubMed](#)]
62. Anger, F.; Klein, I.; Löb, S.; Wiegering, A.; Singh, G.; Sperl, D.; Götze, O.; Geier, A.; Lock, J.F. Preoperative Liver Function Guiding HCC Resection in Normal and Cirrhotic Liver. *Visc. Med.* **2021**, *37*, 94–101. [[CrossRef](#)] [[PubMed](#)]
63. Shin, N.; Choi, J.A.; Choi, J.M.; Cho, E.S.; Kim, J.H.; Chung, J.J.; Yu, J.S. Sclerotic changes of cavernous hemangioma in the cirrhotic liver: Long-term follow-up using dynamic contrast-enhanced computed tomography. *Radiol. Med.* **2020**, *125*, 1225–1232. [[CrossRef](#)] [[PubMed](#)]
64. Petralia, G.; Summers, P.E.; Agostini, A.; Ambrosini, R.; Cianci, R.; Cristel, G.; Calistri, L.; Colagrande, S. Dynamic contrast-enhanced MRI in oncology: How we do it. *Radiol. Med.* **2020**, *125*, 1288–1300. [[CrossRef](#)]
65. Minutoli, F.; Pergolizzi, S.; Blandino, A.; Mormina, E.; Amato, E.; Gaeta, M. Effect of granulocyte colony-stimulating factor on bone marrow: Evaluation by intravoxel incoherent motion and dynamic contrast-enhanced magnetic resonance imaging. *Radiol. Med.* **2020**, *125*, 280–287. [[CrossRef](#)]
66. Ishizawa, T.; Mise, Y.; Aoki, T.; Hasegawa, K.; Beck, Y.; Sugawara, Y.; Kokudo, N. Surgical technique: New advances for expanding indications and increasing safety in liver resection for HCC: The Eastern perspective. *J. Hepatobiliary Pancreat Sci.* **2010**, *17*, 389–393. [[CrossRef](#)]
67. Baker, T.; Tabrizian, P.; Zendejas, I.; Gamblin, T.C.; Kazimi, M.; Boudjema, K.; Geller, D.; Salem, R. Conversion to resection post radioembolization in patients with HCC: Recommendations from a multidisciplinary working group. *HPB* **2021**, S1365-182X(21)01739-1. [[CrossRef](#)]

68. Lee, C.W.; Yu, M.C.; Wang, C.C.; Lee, W.C.; Tsai, H.I.; Kuan, F.C.; Chen, C.W.; Hsieh, Y.C.; Chen, H.Y. Liver resection for hepatocellular carcinoma larger than 10 cm: A multi-institution long-term observational study. *World J. Gastrointest. Surg.* **2021**, *13*, 476–492. [\[CrossRef\]](#)
69. Puijk, R.S.; Ahmed, M.; Adam, A.; Arai, Y.; Arellano, R.; de Baère, T.; Bale, R.; Bellera, C.; Binkert, C.A.; Brace, C.L.; et al. Consensus Guidelines for the Definition of Time-to-Event End Points in Image-guided Tumor Ablation: Results of the SIO and DATECAN Initiative. *Radiology* **2021**, *301*, 533–540. [\[CrossRef\]](#)
70. Ahmed, M.; Solbiati, L.; Brace, C.L.; Breen, D.J.; Callstrom, M.R.; Charboneau, J.W.; Chen, M.H.; Choi, B.I.; de Baère, T.; Gervais, D.A.; et al. Image-guided tumor ablation: Standardization of terminology and reporting criteria—A 10-year update. *Radiology* **2014**, *273*, 241–260. [\[CrossRef\]](#)
71. Ahmed, M. Technology Assessment Committee of the Society of Interventional Radiology. Image-guided tumor ablation: Standardization of terminology and reporting criteria—a 10-year update: Supplement to the consensus document. *J. Vasc. Interv. Radiol.* **2014**, *25*, 1706–1708. [\[CrossRef\]](#) [\[PubMed\]](#)
72. Granata, V.; Grassi, R.; Fusco, R.; Setola, S.V.; Belli, A.; Piccirillo, M.; Pradella, S.; Giordano, M.; Cappabianca, S.; Brunese, L.; et al. Abbreviated MRI Protocol for the Assessment of Ablated Area in HCC Patients. *Int. J. Environ. Res. Public Health* **2021**, *18*, 3598. [\[CrossRef\]](#) [\[PubMed\]](#)
73. Clavien, P.A.; Barkun, J.; de Oliveira, M.L.; Vauthey, J.N.; Dindo, D.; Schulick, R.D.; de Santibañes, E.; Pekolj, J.; Slankamenac, K.; Bassi, C.; et al. The Clavien-Dindo classification of surgical complications: Five-year experience. *Ann. Surg.* **2009**, *250*, 187–196. [\[CrossRef\]](#) [\[PubMed\]](#)
74. Bolliger, M.; Kroehnert, J.A.; Molineus, F.; Kandioler, D.; Schindl, M.; Riss, P. Experiences with the standardized classification of surgical complications (Clavien-Dindo) in general surgery patients. *Eur. Surg.* **2018**, *50*, 256–261. [\[CrossRef\]](#)
75. Katayama, H.; Kurokawa, Y.; Nakamura, K.; Ito, H.; Kanemitsu, Y.; Masuda, N.; Tsubosa, Y.; Satoh, T.; Yokomizo, A.; Fukuda, H.; et al. Extended Clavien-Dindo classification of surgical complications: Japan Clinical Oncology Group postoperative complications criteria. *Surg. Today* **2016**, *46*, 668–685. [\[CrossRef\]](#)
76. Khan, M.T.; Akhtar, T.; Yasin, M.A.; Chaudhary, N.A.; Sadiq, A.; Tameez Ud Din, A. A survey of perioperative complications with Clavien-Dindo classification: A cross-sectional study. *J. Pak. Med. Assoc.* **2021**, *71*, 572–574.
77. Giani, A.; Cipriani, F.; Famularo, S.; Donadon, M.; Bernasconi, D.P.; Ardito, F.; Fazio, F.; Nicolini, D.; Perri, P.; Giuffrida, M.; et al. Performance of Comprehensive Complication Index and Clavien-Dindo Complication Scoring System in Liver Surgery for Hepatocellular Carcinoma. *Cancers* **2020**, *12*, 3868. [\[CrossRef\]](#)
78. Ishii, M.; Mizuguchi, T.; Harada, K.; Ota, S.; Meguro, M.; Ueki, T.; Nishidate, T.; Okita, K.; Hirata, K. Comprehensive review of post-liver resection surgical complications and a new universal classification and grading system. *World J. Hepatol.* **2014**, *6*, 745–751. [\[CrossRef\]](#)
79. Granata, V.; Fusco, R.; Avallone, A.; Cassata, A.; Palaia, R.; Delrio, P.; Grassi, R.; Tatangelo, F.; Grazzini, G.; Izzo, F.; et al. Abbreviated MRI protocol for colorectal liver metastases: How the radiologist could work in pre surgical setting. *PLoS ONE* **2020**, *15*, e0241431. [\[CrossRef\]](#)
80. Albano, D.; Stecco, A.; Micci, G.; Sconfienza, L.M.; Colagrande, S.; Reginelli, A.; Grassi, R.; Carriero, A.; Midiri, M.; Lagalla, R.; et al. Whole-body magnetic resonance imaging (WB-MRI) in oncology: An Italian survey. *Radiol. Med.* **2021**, *126*, 299–305. [\[CrossRef\]](#)
81. Petralia, G.; Zugni, F.; Summers, P.E.; Colombo, A.; Pricolo, P.; Grazioli, L.; Colagrande, S.; Giovagnoni, A.; Padhani, A.R. Italian Working Group on Magnetic Resonance. Whole-body magnetic resonance imaging (WB-MRI) for cancer screening: Recommendations for use. *Radiol. Med.* **2021**, *126*, 1434–1450. [\[CrossRef\]](#) [\[PubMed\]](#)
82. Gurgitano, M.; Angileri, S.A.; Rodà, G.M.; Liguori, A.; Pandolfi, M.; Ierardi, A.M.; Wood, B.J.; Carrafiello, G. Interventional Radiology ex-machina: Impact of Artificial Intelligence on practice. *Radiol. Med.* **2021**, *126*, 998–1006. [\[CrossRef\]](#) [\[PubMed\]](#)
83. Scapicchio, C.; Gabelloni, M.; Barucci, A.; Cioni, D.; Saba, L.; Neri, E. A deep look into radiomics. *Radiol. Med.* **2021**, *126*, 1296–1311. [\[CrossRef\]](#) [\[PubMed\]](#)
84. Stengel, D.; Rademacher, G.; Ekkernkamp, A.; Güthoff, C.; Mutze, S. Emergency ultrasound-based algorithms for diagnosing blunt abdominal trauma. *Cochrane Database Syst. Rev.* **2015**, *2015*, CD004446. [\[CrossRef\]](#)
85. Abdolrazaghnejad, A.; Banaie, M.; Safdari, M. Ultrasonography in Emergency Department; a Diagnostic Tool for Better Examination and Decision-Making. *Adv. J. Emerg. Med.* **2017**, *2*, e7. [\[CrossRef\]](#)
86. Amini, R.; Wyman, M.T.; Hernandez, N.C.; Guisto, J.A.; Adhikari, S. Use of Emergency Ultrasound in Arizona Community Emergency Departments. *J. Ultrasound Med.* **2017**, *36*, 913–921. [\[CrossRef\]](#)
87. Tyler, P.D.; Carey, J.; Stashko, E.; Levenson, R.B.; Shapiro, N.I.; Rosen, C.L. The Potential Role of Ultrasound in the Work-up of Appendicitis in the Emergency Department. *J. Emerg. Med.* **2019**, *56*, 191–196. [\[CrossRef\]](#)
88. Parag, P.; Hardcastle, T.C. Interpretation of emergency CT scans in polytrauma: Trauma surgeon vs. radiologist. *Afr. J. Emerg. Med.* **2020**, *10*, 90–94. [\[CrossRef\]](#)
89. Poletti, P.A.; Andereggen, E.; Rutschmann, O.; de Perrot, T.; Caviezel, A.; Platon, A. Indications au CT low-dose aux urgences [Indications for low-dose CT in the emergency setting]. *Rev. Med. Suisse* **2009**, *5*, 1590–1594.
90. Willeminck, M.J.; Schilham, A.M.; Leiner, T.; Mali, W.P.; de Jong, P.A.; Budde, R.P. Iterative reconstruction does not substantially delay CT imaging in an emergency setting. *Insights Imaging* **2013**, *4*, 391–397. [\[CrossRef\]](#)

91. Ternovoy, S.; Ustyuzhanin, D.; Shariya, M.; Shabanova, M.; Gaman, S.; Serova, N.; Mironov, V.; Merkulova, I.; Rienmueller, A.; Meyer, E.L.; et al. Reliability of coronary computed tomography angiography in acute coronary syndrome in an emergency setting. *Heliyon* **2021**, *7*, e06075. [[CrossRef](#)] [[PubMed](#)]
92. Palumbo, P.; Cannizzaro, E.; Bruno, F.; Schicchi, N.; Fogante, M.; Agostini, A.; De Donato, M.C.; De Cataldo, C.; Giovagnoni, A.; Barile, A.; et al. Coronary artery disease (CAD) extension-derived risk stratification for asymptomatic diabetic patients: Usefulness of low-dose coronary computed tomography angiography (CCTA) in detecting high-risk profile patients. *Radiol. Med.* **2020**, *125*, 1249–1259. [[CrossRef](#)] [[PubMed](#)]
93. Zhang, G.; Yang, Z.; Gong, L.; Jiang, S.; Wang, L.; Zhang, H. Classification of lung nodules based on CT images using squeeze-and-excitation network and aggregated residual transformations. *Radiol. Med.* **2020**, *125*, 374–383. [[CrossRef](#)] [[PubMed](#)]
94. Flammia, F.; Chiti, G.; Trinci, M.; Danti, G.; Cozzi, D.; Grassi, R.; Palumbo, P.; Bruno, F.; Agostini, A.; Fusco, R.; et al. Optimization of CT protocol in polytrauma patients: An update. *Eur. Rev. Med. Pharmacol. Sci.* **2022**, *26*, 2543–2555. [[CrossRef](#)] [[PubMed](#)]
95. Ichikawa, S.; Yamamoto, H.; Morita, T. Comparison of a Bayesian estimation algorithm and singular value decomposition algorithms for 80-detector row CT perfusion in patients with acute ischemic stroke. *Radiol. Med.* **2021**, *126*, 795–803. [[CrossRef](#)]
96. Rampado, O.; Depaoli, A.; Marchisio, F.; Gatti, M.; Racine, D.; Ruggeri, V.; Ruggirello, I.; Darvizeh, F.; Fonio, P.; Ropolo, R. Effects of different levels of CT iterative reconstruction on low-contrast detectability and radiation dose in patients of different sizes: An anthropomorphic phantom study. *Radiol. Med.* **2021**, *126*, 55–62. [[CrossRef](#)]
97. Ruys, A.T.; van Beem, B.E.; Engelbrecht, M.R.; Bipat, S.; Stoker, J.; Van Gulik, T.M. Radiological staging in patients with hilar cholangiocarcinoma: A systematic review and meta-analysis. *Br. J. Radiol.* **2012**, *85*, 1255–1262. [[CrossRef](#)]
98. Ichikawa, S.; Isoda, H.; Shimizu, T.; Tamada, D.; Taura, K.; Togashi, K.; Onishi, H.; Motosugi, U. Distinguishing intrahepatic mass-forming biliary carcinomas from hepatocellular carcinoma by computed tomography and magnetic resonance imaging using the Bayesian method: A bi-center study. *Eur. Radiol.* **2020**, *30*, 5992–6002. [[CrossRef](#)]
99. Chu, H.; Liu, Z.; Liang, W.; Zhou, Q.; Zhang, Y.; Lei, K.; Tang, M.; Cao, Y.; Chen, S.; Peng, S.; et al. Radiomics using CT images for preoperative prediction of futile resection in intrahepatic cholangiocarcinoma. *Eur. Radiol.* **2021**, *31*, 2368–2376. [[CrossRef](#)]
100. Megibow, A.J. Clinical abdominal dual-energy CT: 15 years later. *Abdom. Radiol.* **2020**, *45*, 1198–1201. [[CrossRef](#)]
101. Schicchi, N.; Fogante, M.; Palumbo, P.; Agliata, G.; Esposto Pirani, P.; Di Cesare, E.; Giovagnoni, A. The sub-millisievert era in CTCA: The technical basis of the new radiation dose approach. *Radiol. Med.* **2020**, *125*, 1024–1039. [[CrossRef](#)] [[PubMed](#)]
102. Bozkurt, M.; Eldem, G.; Bozbulut, U.B.; Bozkurt, M.F.; Kılıçkap, S.; Peynircioğlu, B.; Çil, B.; Lay Ergün, E.; Volkan-Salanci, B. Factors affecting the response to Y-90 microsphere therapy in the cholangiocarcinoma patients. *Radiol. Med.* **2021**, *126*, 323–333. [[CrossRef](#)] [[PubMed](#)]
103. Kim, B.H.; Kim, J.S.; Kim, K.H.; Moon, H.J.; Kim, S. Clinical significance of radiation dose-volume parameters and functional status on the patient-reported quality of life changes after thoracic radiotherapy for lung cancer: A prospective study. *Radiol. Med.* **2021**, *126*, 466–473. [[CrossRef](#)] [[PubMed](#)]
104. Mathew, R.P.; Sam, M.; Raubenheimer, M.; Patel, V.; Low, G. Hepatic hemangiomas: The various imaging avatars and its mimickers. *Radiol. Med.* **2020**, *125*, 801–815. [[CrossRef](#)] [[PubMed](#)]
105. Zhang, A.; Song, J.; Ma, Z.; Chen, T. Combined dynamic contrast-enhanced magnetic resonance imaging and diffusion-weighted imaging to predict neoadjuvant chemotherapy effect in FIGO stage IB2-IIA2 cervical cancers. *Radiol. Med.* **2020**, *125*, 1233–1242. [[CrossRef](#)]
106. Sun, N.N.; Ge, X.L.; Liu, X.S.; Xu, L.L. Histogram analysis of DCE-MRI for chemoradiotherapy response evaluation in locally advanced esophageal squamous cell carcinoma. *Radiol. Med.* **2020**, *125*, 165–176. [[CrossRef](#)]
107. Shannon, B.A.; Ahlawat, S.; Morris, C.D.; Levin, A.S.; Fayad, L.M. Do contrast-enhanced and advanced MRI sequences improve diagnostic accuracy for indeterminate lipomatous tumors? *Radiol. Med.* **2022**, *127*, 90–99. [[CrossRef](#)]
108. Lee, J.; Joo, I.; Lee, D.H.; Jeon, S.K.; Lee, J.M. Clinical outcomes of patients with a high alpha-fetoprotein level but without evident recurrence on CT or MRI in surveillance after curative-intent treatment for hepatocellular carcinoma. *Abdom. Radiol.* **2021**, *46*, 597–606. [[CrossRef](#)]
109. Görgec, B.; Hansen, I.; Kemmerich, G.; Syversveen, T.; Abu Hilal, M.; Belt, E.J.T.; Bisschops, R.H.C.; Bollen, T.L.; Bosscha, K.; Burgmans, M.C.; et al. Clinical added value of MRI to CT in patients scheduled for local therapy of colorectal liver metastases (CAMINO): Study protocol for an international multicentre prospective diagnostic accuracy study. *BMC Cancer* **2021**, *21*, 1116. [[CrossRef](#)]
110. Chen, J.; Zhou, J.; Kuang, S.; Zhang, Y.; Xie, S.; He, B.; Deng, Y.; Yang, H.; Shan, Q.; Wu, J.; et al. Liver Imaging Reporting and Data System Category 5: MRI Predictors of Microvascular Invasion and Recurrence After Hepatectomy for Hepatocellular Carcinoma. *AJR Am. J. Roentgenol.* **2019**, *213*, 821–830; Erratum in *AJR Am. J. Roentgenol.* **2019**, *213*, 958. [[CrossRef](#)]
111. Granata, V.; Fusco, R.; Avallone, A.; Filice, F.; Tatangelo, F.; Piccirillo, M.; Grassi, R.; Izzo, F.; Petrillo, A. Critical analysis of the major and ancillary imaging features of LI-RADS on 127 proven HCCs evaluated with functional and morphological MRI: Lights and shadows. *Oncotarget* **2017**, *8*, 51224–51237. [[CrossRef](#)] [[PubMed](#)]
112. Granata, V.; Fusco, R.; Avallone, A.; Catalano, O.; Filice, F.; Leongito, M.; Palaia, R.; Izzo, F.; Petrillo, A. Major and ancillary magnetic resonance features of LI-RADS to assess HCC: An overview and update. *Infect. Agent Cancer* **2017**, *12*, 23. [[CrossRef](#)] [[PubMed](#)]



113. Granata, V.; Fusco, R.; Setola, S.V.; Picone, C.; Vallone, P.; Belli, A.; Incollingo, P.; Albino, V.; Tatangelo, F.; Izzo, F.; et al. Microvascular invasion and grading in hepatocellular carcinoma: Correlation with major and ancillary features according to LIRADS. *Abdom. Radiol.* **2019**, *44*, 2788–2800. [[CrossRef](#)] [[PubMed](#)]
114. Katz, L.H.; Benjaminov, O.; Belinki, A.; Geler, A.; Braun, M.; Knizhnik, M.; Aizner, S.; Shaharabani, E.; Sulkes, J.; Shabtai, E.; et al. Magnetic resonance cholangiopancreatography for the accurate diagnosis of biliary complications after liver transplantation: Comparison with endoscopic retrograde cholangiography and percutaneous transhepatic cholangiography-long-term follow-up. *Clin. Transplant.* **2010**, *24*, E163–E169. [[CrossRef](#)]
115. Letourneau, J.G.; Steely, J.W.; Crass, J.R.; Goldberg, M.E.; Grage, T.; Day, D.L. Upper abdomen: CT findings following partial hepatectomy. *Radiology* **1988**, *166 Pt 1*, 139–141. [[CrossRef](#)] [[PubMed](#)]
116. Patrone, R.; Granata, V.; Belli, A.; Palaia, R.; Albino, V.; Piccirillo, M.; Fusco, R.; Tatangelo, F.; Nasti, G.; Avallone, A.; et al. The safety and efficacy of Glubran 2 as biliostatic agent in liver resection. *Infect. Agent Cancer* **2021**, *16*, 19. [[CrossRef](#)]
117. De Filippo, M.; Puglisi, S.; D’Amuri, F.; Gentili, F.; Paladini, I.; Carrafiello, G.; Maestroni, U.; Del Rio, P.; Ziglioli, F.; Pagnini, F. CT-guided percutaneous drainage of abdominopelvic collections: A pictorial essay. *Radiol. Med.* **2021**, *126*, 1561–1570. [[CrossRef](#)]
118. Cannataci, C.; Cimo, B.; Mamone, G.; Tuzzolino, F.; D’Amico, M.; Cortis, K.; Maruzzelli, L.; Miraglia, R. Portal vein puncture-related complications during transjugular intrahepatic portosystemic shunt creation: Colapinto needle set vs. Rösch-Uchida needle set. *Radiol. Med.* **2021**, *126*, 1487–1495. [[CrossRef](#)]
119. Mahnken, A.H.; Boulosa Seoane, E.; Cannavale, A.; de Haan, M.W.; Dezman, R.; Kloeckner, R.; O’Sullivan, G.; Ryan, A.; Tsoumakidou, G. CIRSE Clinical Practice Manual. *Cardiovasc. Intervent. Radiol.* **2021**, *44*, 1323–1353; Erratum in *Cardiovasc. Intervent. Radiol.* **2021**, *44*, 1323–1353. [[CrossRef](#)]
120. Miele, V.; Di Giampietro, I. Diagnostic Imaging in Emergency. *Salut. E Soc.* **2014**, 127–138. [[CrossRef](#)]
121. De Cecco, C.N.; Buffa, V.; Fedeli, S.; Luzietti, M.; Vallone, A.; Ruopoli, R.; Miele, V.; Rengo, M.; Maurizi Enrici, M.; Fina, P.; et al. Preliminary experience with abdominal dual-energy CT (DECT): True versus virtual nonenhanced images of the liver. *Radiol. Med.* **2010**, *115*, 1258–1266. [[CrossRef](#)] [[PubMed](#)]
122. Di Giacomo, V.; Trinci, M.; van der Byl, G.; Catania, V.D.; Calisti, A.; Miele, V. Ultrasound in newborns and children suffering from non-traumatic acute abdominal pain: Imaging with clinical and surgical correlation. *J. Ultrasound* **2014**, *18*, 385–393. [[CrossRef](#)] [[PubMed](#)]
123. Izzo, F.; Palaia, R.; Albino, V.; Amore, A.; di Giacomo, R.; Piccirillo, M.; Leongito, M.; Nasto, A.; Granata, V.; Petrillo, A.; et al. Hepatocellular carcinoma and liver metastases: Clinical data on a new dual-lumen catheter kit for surgical sealant infusion to prevent perihepatic bleeding and dissemination of cancer cells following biopsy and loco-regional treatments. *Infect. Agent Cancer* **2015**, *10*, 11. [[CrossRef](#)] [[PubMed](#)]
124. Rahbari, N.N.; Garden, O.J.; Padbury, R.; Maddern, G.; Koch, M.; Hugh, T.J.; Fan, S.T.; Nimura, Y.; Figueras, J.; Vauthey, J.N.; et al. Post-hepatectomy haemorrhage: A definition and grading by the International Study Group of Liver Surgery (ISGLS). *HPB* **2011**, *13*, 528–535. [[CrossRef](#)] [[PubMed](#)]
125. Lubner, M.; Menias, C.; Rucker, C.; Bhalla, S.; Peterson, C.M.; Wang, L.; Gratz, B. Blood in the belly: CT findings of hemoperitoneum. *Radiographics* **2007**, *27*, 109–125. [[CrossRef](#)] [[PubMed](#)]
126. Ilyas, M.; Bashir, M.; Robbani, I.; Rasool, S.R.; Shera, F.A.; Hamid, I. Sentinel clot sign in hemoperitoneum. *Abdom. Radiol.* **2019**, *44*, 1955–1956. [[CrossRef](#)]
127. Shanmuganathan, K.; Mirvis, S.E.; Reaney, S.M. Pictorial review: CT appearances of contrast medium extravasations associated with injury sustained from blunt abdominal trauma. *Clin. Radiol.* **1995**, *50*, 182–187. [[CrossRef](#)] [[PubMed](#)]
128. Byun, J.; Kim, K.W.; Lee, J.; Kwon, H.J.; Kwon, J.H.; Song, G.W.; Lee, S.G. The role of multiphase CT in patients with acute postoperative bleeding after liver transplantation. *Abdom. Radiol.* **2020**, *45*, 141–152. [[CrossRef](#)]
129. Di Domenico, S.; Rossini, A.; Petrocelli, F.; Valente, U.; Ferro, C. Recurrent acute Budd-Chiari syndrome after right hepatectomy: US color-Doppler vascular pattern and left hepatic vein stenting for treatment. *Abdom. Imaging* **2013**, *38*, 320–323. [[CrossRef](#)]
130. Yoshiya, S.; Shirabe, K.; Nakagawara, H.; Soejima, Y.; Yoshizumi, T.; Ikegami, T.; Yamashita, Y.; Harimoto, N.; Nishie, A.; Yamanaka, T.; et al. Portal vein thrombosis after hepatectomy. *World J. Surg.* **2014**, *38*, 1491–1497. [[CrossRef](#)]
131. Cohen, J.; Edelman, R.R.; Chopra, S. Portal vein thrombosis: A review. *Am. J. Med.* **1992**, *92*, 173–182. [[CrossRef](#)]
132. Witte, C.L.; Brewer, M.L.; Witte, M.H.; Pond, G.B. Protean manifestations of pylethrombosis. A review of thirty-four patients. *Ann. Surg.* **1985**, *202*, 191–202. [[CrossRef](#)] [[PubMed](#)]
133. Sheen, C.L.; Lamparelli, H.; Milne, A.; Green, I.; Ramage, J.K. Clinical features, diagnosis and outcome of acute portal vein thrombosis. *QJM* **2000**, *93*, 531–534. [[CrossRef](#)] [[PubMed](#)]
134. Sakuraba, M.; Miyamoto, S.; Nagamatsu, S.; Kayano, S.; Taji, M.; Kinoshita, T.; Kosuge, T.; Kimata, Y. Hepatic artery reconstruction following ablative surgery for hepatobiliary and pancreatic malignancies. *Eur. J. Surg. Oncol.* **2012**, *38*, 580–585. [[CrossRef](#)]
135. Silva, M.A.; Jambulingam, P.S.; Gunson, B.K.; Mayer, D.; Buckels, J.A.; Mirza, D.F.; Bramhall, S.R. Hepatic artery thrombosis following orthotopic liver transplantation: A 10-year experience from a single centre in the United Kingdom. *Liver Transpl.* **2006**, *12*, 146–151. [[CrossRef](#)]
136. Bhattacharjya, S.; Gunson, B.K.; Mirza, D.F.; Mayer, D.A.; Buckels, J.A.; McMaster, P.; Neuberger, J.M. Delayed hepatic artery thrombosis in adult orthotopic liver transplantation—A 12-year experience. *Transplantation* **2001**, *71*, 1592–1596. [[CrossRef](#)]
137. McNaughton, D.A.; Abu-Yousef, M.M. Doppler US of the liver made simple. *Radiographics* **2011**, *31*, 161–188; Erratum in *Radiographics* **2011**, *31*, 904. [[CrossRef](#)]

138. Ralls, P.W.; Johnson, M.B.; Radin, D.R.; Boswell, W.D., Jr.; Lee, K.P.; Halls, J.M. Budd-Chiari syndrome: Detection with color Doppler sonography. *AJR Am. J. Roentgenol.* **1992**, *159*, 113–116. [[CrossRef](#)]
139. Rahbari, N.N.; Garden, O.J.; Padbury, R.; Brooke-Smith, M.; Crawford, M.; Adam, R.; Koch, M.; Makuuchi, M.; Dematteo, R.P.; Christophi, C.; et al. Posthepatectomy liver failure: A definition and grading by the International Study Group of Liver Surgery (ISGLS). *Surgery* **2011**, *149*, 713–724. [[CrossRef](#)]
140. Boonstra, E.A.; de Boer, M.T.; Sieders, E.; Peeters, P.M.; de Jong, K.P.; Slooff, M.J.; Porte, R.J. Risk factors for central bile duct injury complicating partial liver resection. *Br. J. Surg.* **2012**, *99*, 256–262. [[CrossRef](#)]
141. Hoeffel, C.; Azizi, L.; Lewin, M.; Laurent, V.; Aubé, C.; Arrivé, L.; Tubiana, J.M. Normal and pathologic features of the postoperative biliary tract at 3D MR cholangiopancreatography and MR imaging. *Radiographics* **2006**, *26*, 1603–1620. [[CrossRef](#)] [[PubMed](#)]
142. Yamashita, Y.; Hamatsu, T.; Rikimaru, T.; Tanaka, S.; Shirabe, K.; Shimada, M.; Sugimachi, K. Bile leakage after hepatic resection. *Ann. Surg.* **2001**, *233*, 45–50. [[CrossRef](#)] [[PubMed](#)]
143. Nagano, Y.; Togo, S.; Tanaka, K.; Masui, H.; Endo, I.; Sekido, H.; Nagahori, K.; Shimada, H. Risk factors and management of bile leakage after hepatic resection. *World J. Surg.* **2003**, *27*, 695–698. [[CrossRef](#)] [[PubMed](#)]
144. Park, M.S.; Kim, K.W.; Yu, J.S.; Kim, M.J.; Kim, K.W.; Lim, J.S.; Cho, E.S.; Yoon, D.S.; Kim, T.K.; Lee, S.I.; et al. Early biliary complications of laparoscopic cholecystectomy: Evaluation on T2-weighted MR cholangiography in conjunction with mangafodipir trisodium-enhanced 3D T1-weighted MR cholangiography. *AJR Am. J. Roentgenol.* **2004**, *183*, 1559–1566. [[CrossRef](#)] [[PubMed](#)]
145. Alegre Castellanos, A.; Molina Granados, J.F.; Escribano Fernandez, J.; Gallardo Muñoz, I.; Triviño Tarradas Fde, A. Early phase detection of bile leak after hepatobiliary surgery: Value of Gd-EOB-DTPA-enhanced MR cholangiography. *Abdom. Imaging* **2012**, *37*, 795–802. [[CrossRef](#)] [[PubMed](#)]
146. Melamud, K.; LeBedis, C.A.; Anderson, S.W.; Soto, J.A. Biliary imaging: Multimodality approach to imaging of biliary injuries and their complications. *Radiographics* **2014**, *34*, 613–623. [[CrossRef](#)] [[PubMed](#)]
147. Thompson, C.M.; Saad, N.E.; Quazi, R.R.; Darcy, M.D.; Picus, D.D.; Menias, C.O. Management of iatrogenic bile duct injuries: Role of the interventional radiologist. *Radiographics* **2013**, *33*, 117–134. [[CrossRef](#)]
148. Kaufman, J.A.; Lee, M.J. *Vascular and Interventional Radiology*; Elsevier Health Sciences: Philadelphia, PA, USA, 2013.
149. Mulé, S.; Colosio, A.; Cazejust, J.; Kianmanesh, R.; Soyer, P.; Hoeffel, C. Imaging of the postoperative liver: Review of normal appearances and common complications. *Abdom. Imaging* **2015**, *40*, 2761–2776. [[CrossRef](#)]
150. Hwang, J.; Kim, S.H.; Lee, M.W.; Lee, J.Y. Small ( $\leq 2$  cm) hepatocellular carcinoma in patients with chronic liver disease: Comparison of gadoteric acid-enhanced 3.0 T MRI and multiphasic 64-multirow detector CT. *Br. J. Radiol.* **2012**, *85*, e314–e322. [[CrossRef](#)]
151. Granata, V.; Fusco, R.; Setola, S.V.; Castelguidone, E.L.D.; Camera, L.; Tafuto, S.; Avallone, A.; Belli, A.; Incollingo, P.; Palaia, R.; et al. The multidisciplinary team for gastroenteropancreatic neuroendocrine tumours: The radiologist's challenge. *Radiol. Oncol.* **2019**, *53*, 373–387. [[CrossRef](#)]
152. Danti, G.; Flammia, F.; Matteuzzi, B.; Cozzi, D.; Berti, V.; Grazzini, G.; Pradella, S.; Recchia, L.; Brunese, L.; Miele, V. Gastrointestinal neuroendocrine neoplasms (GI-NENs): Hot topics in morphological, functional, and prognostic imaging. *Radiol. Med.* **2021**, *126*, 1497–1507. [[CrossRef](#)] [[PubMed](#)]
153. Park, S.H.; Kim, Y.S.; Choi, J. Dosimetric analysis of the effects of a temporary tissue expander on the radiotherapy technique. *Radiol. Med.* **2021**, *126*, 437–444. [[CrossRef](#)] [[PubMed](#)]
154. Granata, V.; Fusco, R.; De Muzio, F.; Cutolo, C.; Setola, S.V.; Dell'Aversana, F.; Belli, A.; Romano, C.; Ottaiano, A.; Nasti, G.; et al. Magnetic Resonance Features of Liver Mucinous Colorectal Metastases: What the Radiologist Should Know. *J. Clin. Med.* **2022**, *11*, 2221. [[CrossRef](#)] [[PubMed](#)]
155. Cutolo, C.; Dell'Aversana, F.; Fusco, R.; Grazzini, G.; Chiti, G.; Simonetti, I.; Bruno, F.; Palumbo, P.; Pierpaoli, L.; Valeri, T.; et al. Combined Hepatocellular-Cholangiocarcinoma: What the Multidisciplinary Team Should Know. *Diagnostics* **2022**, *12*, 890. [[CrossRef](#)]
156. Granata, V.; Fusco, R.; Belli, A.; Borzillo, V.; Palumbo, P.; Bruno, F.; Grassi, R.; Ottaiano, A.; Nasti, G.; Pilone, V.; et al. Conventional, functional and radiomics assessment for intrahepatic cholangiocarcinoma. *Infect. Agent Cancer* **2022**, *17*, 13. [[CrossRef](#)]
157. Patrone, R.; Izzo, F.; Palaia, R.; Granata, V.; Nasti, G.; Ottaiano, A.; Pasta, G.; Belli, A. Minimally invasive surgical treatment of intrahepatic cholangiocarcinoma: A systematic review. *World J. Gastrointest Oncol.* **2021**, *13*, 2203–2215. [[CrossRef](#)]
158. Kim, K.A.; Kim, M.J.; Choi, J.Y.; Park, M.S.; Lim, J.S.; Chung, Y.E.; Kim, K.W. Detection of recurrent hepatocellular carcinoma on post-operative surveillance: Comparison of MDCT and gadoteric acid-enhanced MRI. *Abdom. Imaging* **2014**, *39*, 291–299. [[CrossRef](#)]
159. Sasaki, K.; Matsuda, M.; Ohkura, Y.; Kawamura, Y.; Inoue, M.; Hashimoto, M.; Ikeda, K.; Kumada, H.; Watanabe, G. In hepatocellular carcinomas, any proportion of poorly differentiated components is associated with poor prognosis after hepatectomy. *World J. Surg.* **2014**, *38*, 1147–1153. [[CrossRef](#)]
160. Hyder, O.; Hatzaras, I.; Sotiropoulos, G.C.; Paul, A.; Alexandrescu, S.; Marques, H.; Pulitano, C.; Barroso, E.; Clary, B.M.; Aldrighetti, L.; et al. Recurrence after operative management of intrahepatic cholangiocarcinoma. *Surgery* **2013**, *153*, 811–818. [[CrossRef](#)]

161. Jadvar, H.; Henderson, R.W.; Conti, P.S. [F-18]fluorodeoxyglucose positron emission tomography and positron emission tomography: Computed tomography in recurrent and metastatic cholangiocarcinoma. *J. Comput. Assist. Tomogr.* **2007**, *31*, 223–228. [[CrossRef](#)]
162. de Jong, M.C.; Pulitano, C.; Ribero, D.; Strub, J.; Mentha, G.; Schulick, R.D.; Choti, M.A.; Aldrighetti, L.; Capussotti, L.; Pawlik, T.M. Rates and patterns of recurrence following curative intent surgery for colorectal liver metastasis: An international multi-institutional analysis of 1669 patients. *Ann. Surg.* **2009**, *250*, 440–448. [[CrossRef](#)] [[PubMed](#)]
163. DeMatteo, R.P.; Palese, C.; Jarnagin, W.R.; Sun, R.L.; Blumgart, L.H.; Fong, Y. Anatomic segmental hepatic resection is superior to wedge resection as an oncologic operation for colorectal liver metastases. *J. Gastrointest Surg.* **2000**, *4*, 178–184. [[CrossRef](#)]
164. Ward, J.; Sheridan, M.B.; Guthrie, J.A.; Davies, M.H.; Millson, C.E.; Lodge, J.P.; Pollard, S.G.; Prasad, K.R.; Toogood, G.J.; Robinson, P.J. Bile duct strictures after hepatobiliary surgery: Assessment with MR cholangiography. *Radiology* **2004**, *231*, 101–108. [[CrossRef](#)] [[PubMed](#)]
165. Bowie, J.D. What is the upper limit of normal for the common bile duct on ultrasound: How much do you want it to be? *Am. J. Gastroenterol.* **2000**, *95*, 897–900. [[CrossRef](#)]
166. Granata, V.; Fusco, R.; Filice, S.; Catalano, O.; Piccirillo, M.; Palaia, R.; Izzo, F.; Petrillo, A. The current role and future perspectives of functional parameters by diffusion weighted imaging in the assessment of histologic grade of HCC. *Infect. Agent Cancer* **2018**, *13*, 23. [[CrossRef](#)]
167. Granata, V.; Petrillo, M.; Fusco, R.; Setola, S.V.; de Lutio di Castelguidone, E.; Catalano, O.; Piccirillo, M.; Albino, V.; Izzo, F.; Petrillo, A. Surveillance of HCC Patients after Liver RFA: Role of MRI with Hepatospecific Contrast versus Three-Phase CT Scan-Experience of High Volume Oncologic Institute. *Gastroenterol. Res. Pract.* **2013**, *2013*, 469097. [[CrossRef](#)]
168. Rega, D.; Pace, U.; Scala, D.; Chiodini, P.; Granata, V.; Fares Bucci, A.; Pecori, B.; Delrio, P. Treatment of splenic flexure colon cancer: A comparison of three different surgical procedures: Experience of a high volume cancer center. *Sci. Rep.* **2019**, *9*, 10953. [[CrossRef](#)]
169. Izzo, F.; Piccirillo, M.; Albino, V.; Palaia, R.; Belli, A.; Granata, V.; Setola, S.; Fusco, R.; Petrillo, A.; Orlando, R.; et al. Prospective screening increases the detection of potentially curable hepatocellular carcinoma: Results in 8900 high-risk patients. *HPB* **2013**, *15*, 985–990. [[CrossRef](#)]
170. Barretta, M.L.; Catalano, O.; Setola, S.V.; Granata, V.; Marone, U.; D’Errico Gallipoli, A. Gallbladder metastasis: Spectrum of imaging findings. *Abdom. Imaging* **2011**, *36*, 729–734. [[CrossRef](#)]